Adaptive radiation therapy treatment for patients with locally advanced non-small cell lung cancer

Tuva Borgund Johannessen

Supervisors: Liv B. Hysing and Vilde Ragnvaldsen

Master thesis in medical physics

Department of Physics and Technology

University of Bergen

June 2023

Acknowledgements

First of all, I would like to express my sincere gratitude to my supervisor Liv Bolstad Hysing and co-supervisor Vilde Ragnvaldsen for guiding me throughout this semester. Your support and feedback have been extremely valuable, and thank you for your dedication throughout this project.

Thank you Liv, for introducing me to this interesting project and your encouragement. Our conversations always resulted in endless possibilities regarding this thesis, and motivated me to give my very best. Your expertise has been inspiring and helpful. Thank you Vilde, for all your help with SPSS and Eclipse, useful literature and knowledge. Your positive attitude has been motivating when the workload has felt overwhelming. I also need to thank the rest of the people in Haukelandsbakken for your welcoming environment.

Thanks to all of my friends and fellow students at UiB, for making these five years memorable both academically and socially. Special thanks to Karoline, Beate and Hanne. Our friendship has been very important to me, and I am looking forward to making more memories.

I would also like to thank my big and caring family for always being there for me and supporting me throughout the years of study. Finally, I must express my gratitude towards my patient and loving partner Joachim. This would have been hard without your support.

Tuva Borgund Johannessen

Bergen, June 2023

Abstract

Introduction and aim: For locally advanced non-small cell lung cancer (LA-NSCLC) the current state-of-the-art treatment is intensity modulated radiation therapy (IMRT) using photons. Radiation therapy of LA-NSCLC can be challenging because of anatomical changes in the treatment region, and there is an increased risk of missing the treatment target and irradiating healthy tissue. Adaptive radiation therapy (ART) has the potential to improve the treatment by adjusting it for uncertainties like this. The purpose of this thesis was to investigate the dosimetric impact of anatomical changes over the course of the treatment, and studying how well the HUH traffic light protocol worked for identifying these changes.

Method: Forty-one LA-NSCLC patients primarily treated with photon IMRT (60 or 66 Gy by 2 Gy per fraction) were included in the study, and anatomical changes present had been registered following the traffic light protocol. Recalculating the original treatment plan onto CT scans made it possible to evaluate dosimetric variation between planning, and the first and third week of treatment, by studying target volume and organs at risk (OAR). Patients receiving tumor-match treatment as a result from the protocol, were studied further by recalculating based on tumor-match instead of bone-match alignment as initially conducted.

Results: Target coverage was significantly better at planning compared to the first and third week of treatment, and 19/79 recalculations resulted in CTV V95% < 99%. Of these 19 recalculations, 17 were identified by the protocol with a degree of anatomical change. All replan adaptations made based on the protocol resulted in better target coverage but jeopardized healthy tissue. Tumor-match had no overall significant impact on the target coverage, and only 4/21 tumor-match treatments were beneficial based on our results.

Conclusion: Patients who were at risk of low target coverage got detected by the HUH traffic light protocol, but proper protocol training was necessary. Impacts for OAR dosage was too complex to anticipate by the protocol, and this needs further research for patients prone to overdosage of OARs.

Contents

Abbreviations

3DCT Three-Dimensional Computed Tomography
4DCT Four-Dimensional Computed Tomography
AIP Average Intensity Projection
ART Adaptive Radiation Therapy
BSRT Breathing Synchronized Radiotherapy
CBCT Cone Beam Computed Tomography
CT Computed Tomography
CTV Clinical Target Volume
DIBH Deep Inspiration Breath Hold
DVH Dose Volume Histogram
FDG Fluoro-2-Deoxy-Glucose
GTV Gross Tumor Volume
HU Hounsfield Unit
HUH Haukeland University Hospital
IGRT Image Guided Radiation Therapy
iGTV Internal Gross Tumor Volume
IMRT Intensity Modulated Radiation Therapy
IQR Interquartile range
ITAC Intra Thoracic Anatomical Change
LA Locally Advanced
LINAC Linear Accelerator
MLC Multileaf Collimator
MRI Magnetic Resonance Imaging
MU Monitor Unit
NSCLC Non-Small Cell Lung Cancer
NTCP Normal Tissue Complication Probability
OAR Organs At Risk
pCT Planning Computed Tomography
PET Positron Emission Tomography
PTV Planning Target Volume
QA Quality Assurance
rCT Repeated Computed Tomography
RTT Radiation Therapy Technologist
SCLC Small Cell Lung Cancer
SPECT Single-Photon Emission Computed Tomography
TCP Tumor Control Probability
VMAT Volumetric Modulated Arc Therapy
VOI Volume Of Interest

List of figures

List of tables

1 Introduction

GLOBOCAN 2020 estimation of cancer incidence and mortality worldwide shows that lung cancer is the second most commonly diagnosed cancer, just surpassed by female breast cancer [1]. Lung cancer still remains the type of cancer with most deaths in 2020 worldwide, with 1.8 million deaths (18%) estimated. Non-small cell lung cancer (NSCLC) is the most frequent type of lung cancer. When the tumor has not spread to distant body parts, only to nearby tissue or lymph nodes, it can be referred to as Locally Advanced (LA). For untreated LA-NSCLC the prognoses of 2 years survival are as low as 0-4% [2].

The prognosis for NSCLC is poor overall, but it depends on the staging at the time of detection. About 40% of all NSCLC is Locally Advanced with stage III by the time of diagnosis [3]. Patients with stage III NSCLC are often inoperable, so radiotherapy, chemotherapy, and immunotherapy are the main choices of treatment. Radiotherapy uses radiation to damage cancer cells, but in addition the radiation might damage healthy tissue. To avoid this as much as possible, there are different treatment methods developed. Radiation treatments are usually delivered with photons in Norway, and the state-of-the-art modality for lung cancer is intensity modulated radiation therapy (IMRT). This thesis focuses on IMRT treatment of stage III LA-NSCLC using photons.

Radiotherapy of LA-NSCLC is challenging because of uncertainties during the treatment caused by inter-fractional anatomical changes and breathing motion [4]. Due to these uncertainties, the delivered radiotherapy treatment is often degraded in quality compared to the planned treatment. There is a risk of reduced tumor coverage and increased irradiation to parts of the body we want to avoid. So, as well as the treatment quality gets lowered, the risk of severe side effects increases. Esophagitis with difficulties of swallowing may occur after treatment, and radiation induced pneumonitis and fibrosis can develop as late effects [2].

It is important to develop methods that counter these uncertainties, to increase overall survival for this patient group. A good multidisciplinary team is needed for an optimal treatment of LA-NSCLC, due to the big heterogeneity for the disease [2]. The pulmDIBH study by Haukeland University Hospital (HUH) in Bergen, has a main goal to develop better and more tailored radiotherapy for this patient group. Adaptive radiation therapy (ART) aims to adjust the treatment plan during the treatment course to avoid normal tissue complications and ensure target coverage. A part of the pulmDIBH study was to implement a traffic-light protocol as part of an off-line adaptive method, where anatomical changes are reported during the treatment course.

1.1 Project objectives and motivation

This thesis is a part of the pulmDIBH research project, and the motivation behind is based on improvement of ART for LA-NSCLC patients. Improvement of ART for these patients, might increase the overall survival. The aim of the thesis was to determine the impacts of anatomical changes for the delivered dose. By recalculating the original treatment plan onto CT scans taken the first and third week of treatment, the dose distribution during the treatment course was evaluated. How well the HUH traffic light protocol functioned, was evaluated by studying the dose distributions from the recalculations compared to the anatomical changes reported at the time of the CT scans.

The thesis will attempt to answer these research questions:

- How does anatomical changes impact on target coverage and dose to healthy tissue?
- Does the traffic light protocol detect anatomical changes and identify the patient's need for adaptation?

2 Theory

2.1 Lung anatomy

Lungs are two cone-shaped organs in the chest that transfers oxygen into the body when breathing (figure 2.1). When release of breath, the lungs let go of carbon dioxide as a waste product of the body's cells. The right lung is bigger than the left and has three lobes, while the left lung has two lobes. When we breathe the air travels down the trachea and further through two bronchi leading the air to both lungs [5].

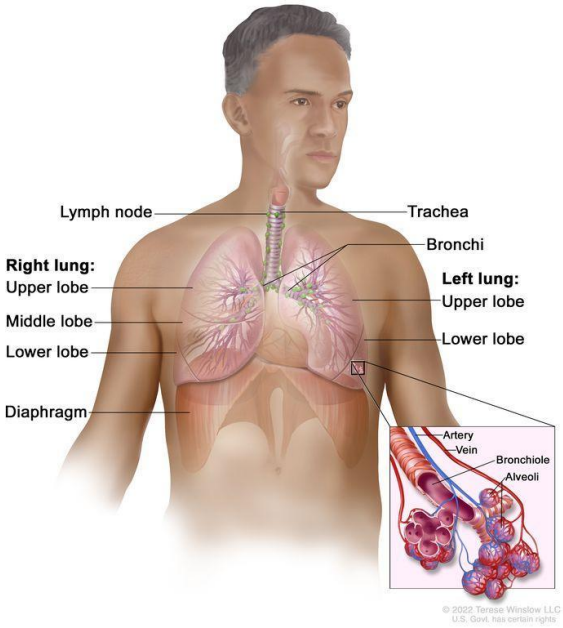

Figure 2.1: Anatomy of the lungs [5]

The two bronchi further branch into multiple and smaller pathways, called bronchioles [5, 6]. The terminal bronchioles branch into alveoli, where oxygen is transferred to the bloodstream. The lung's concave base rests on the diaphragm. The lobes contain airways, arteries, and veins. Both lungs are covered in a surface of cells that is called *visceral pleural*. The pleural space contains pleural fluid that allows mobility of the lung while we breathe [7].

2.2 Lung Cancer

There is coexistence of cells and tissue that make up different parts of our body, which communicates and does their assigned task. Normally these cells grow and die in a specific cycle, but the cycle can change and result in an increased number of cells if there are mutations in the genes. The increased number of cells can form into malignant tumors that can spread to other tissue, and this is what we call cancer. It is not necessarily a big contrast between cancerous cells and normal cells, and the proliferation can be slow or rapid. Cancer cells do not follow the rules of function and structure that govern normal cells and tissues within a certain tissue. Cancer distinguishes from normal cells, and other abnormal cellular growths, in its characteristic independence and ability to ignore anatomic barriers. [8].

The tumor originates in one part of the body, like one of the lungs, but can also spread to other parts of the body. This is called metastasis, and the cancer cells travel through blood or the lymph system away from the primary tumor [5]. The development of lung cancer cases is primarily a result of smoking habits through the years [9]. Earlier, smoking was more common by men, and they started smoking at a younger age. Eight out of 10 lung cancer cases are due to use of tobacco, and that is why lung cancer is one of the most easily preventable forms of cancer. But there are still cases of lung cancer patients who have never touched a cigarette.

2.2.2 Non-small Cell Lung Cancer

Non-small cell lung cancer (NSCLC) and small cell lung cancer (SCLC) are the two main types of lung cancer. NSCLC dominates with 85% of the patients, while the remaining 15% are diagnosed with SCLC [10]. The difference between the two cancer forms is mainly where the cancer begins, the way it progresses, and the structure of the cells when you study them under a microscope [11]. As the name implies, the cancer cells of SCLC are smaller than normal cells and cells of NSCLC. SCLC is also a more aggressive cancer form that grows rapidly and spreads more easily. The patients studied in this thesis are diagnosed with NSCLC.

At what stage the diagnosis is discovered is directly related to the clinical outcome for NSCLC, which means that a screening modality that allows detection is important [10]. Annual low dose computed tomography (CT) screening of the chest for high-risk individuals is recommended by the US Preventive Services Task Force. The recommendation is for individuals with a smoking history of 30 years, between the ages of 55 to 80 years. The

European Commission recommends producing a lung cancer screening program for high-risk citizens at the age 50-75 [12]. Here in Norway, there is no funded screening program yet. However, there has been a pilot project funded by The Norwegian Cancer Society in 2022 which maps out how many Norwegians that are in the risk group and how many that would be interested in a screening program [3, 13].

In general, the procedures for determination of the presence of NSCLC are physical examination, history, routine laboratory evaluations, chest x-ray, chest CT-scan with contrast material infused, and biopsy [14]. It can be difficult to separate symptoms of lung cancer from other malignant diseases, and the x-ray image can be a quick and useful way to expose the suspicion [3]. The patient will then be further examined by a lung specialist, and CT with contrast material is carried out for the thorax and abdomen. The CT scanner consists of a cone beam that makes projections around the patient and the scanner collects transmission measurements of x-rays through the patient [15]. A tomographic picture can then be reconstructed from the measured transmission data. The image is detailed of the body's anatomical structures made by the x-ray slices of the body. Still, the CT may miss small or early-stage tumors.

Another limitation in comparison to other imaging modalities, is that CT does not provide functional information of the tumor. Positron emission tomography (PET) documents physiologic abnormalities, or changes in metabolism, by ejecting a radioactive tracer into the patient [16]. PET with [^{18}F]-fluoro-2-deoxy-glucose (FDG) tracers should be used when examining patients with LA-NSCLC [3]. The amount of FDG different cells take up depends on their metabolic activity, and most tumors have high uptake of glucose and will attract most of the tracer. A detector will detect the position, when a photon pair is emitted from where the tracer is located [16]. PET can further be used to decide the stage of the patient's cancer [3]. The majority of patients studied in this thesis have stage III NSCLC, and in the next chapter the staging system of NSCLC is described.

2.2.3 TNM for stage III NSCLC

NSCLC follows the TNM staging system, which is based on three categories: tumor, node and metastasis [17]. Tumor size of the primary tumor is considered and if it has grown into surrounding structures. Lymph nodes are contributing to the body`s immune and circulatory systems. They are small structures and the regional lymph nodes (lymph nodes in the region of the tumor) can be affected by the cancer. It also needs to be considered if there is distant metastasis in other distant organs such as the other lung, bones, brain, or distant lymph nodes. The severity and combinations of these three factors determine the patient's stage. The TNM classification as a guideline contributes to a better global cancer control, and has a purpose both for the patient and for research activity [18]. The patients studied in this thesis are mainly diagnosed with stage III NSCLC, and the subgroups of stage III NSCLC are represented in table 2.1. As seen from table 2.1, there is no distant metastasis for stage III NSCLC, and for NSCLC this only occurs for stage IV patients [19]. Sometimes, and hereby in this thesis, stage III NSCLC is referred to as locally advanced (LA-NSCLC).

Table 2.1: Subsections of stage III NSCLC: IIA, IIB, IIC represented with the TNM staging system. Table gathered from [19]. See appendix A for explanations for the abbreviations.

Stage IIIA	T1a-c, T2a-b	N2	M0
	T3	N1	M0
	T4	N0, N1	M0
Stage IIIB	T1a-c, T2a-b	N3	M0
	T3, T4	N2	M0
Stage IIIC	T3, T4	N3	M0

There are many combinations of tumor size and possible spread to lymph nodes for stage III NSCLC. Figure 2.2 illustrates an example of stage IIIB NSCLC, where the tumor is larger than 5 cm in greatest dimension, with spread to mediastinal lymph nodes near the primary tumor, and tumors have grown into the outer lining or cases of growth described in the figure [17]. IIIB NSCLC can also have a tumor smaller than 5 cm in the greatest dimension, but with spread to the mediastinal or hilar nodes, but not near the primary tumor. In that case tumors may or may not have grown into the main bronchus or the lungs inner lining, or have caused swelling or lung collapse.

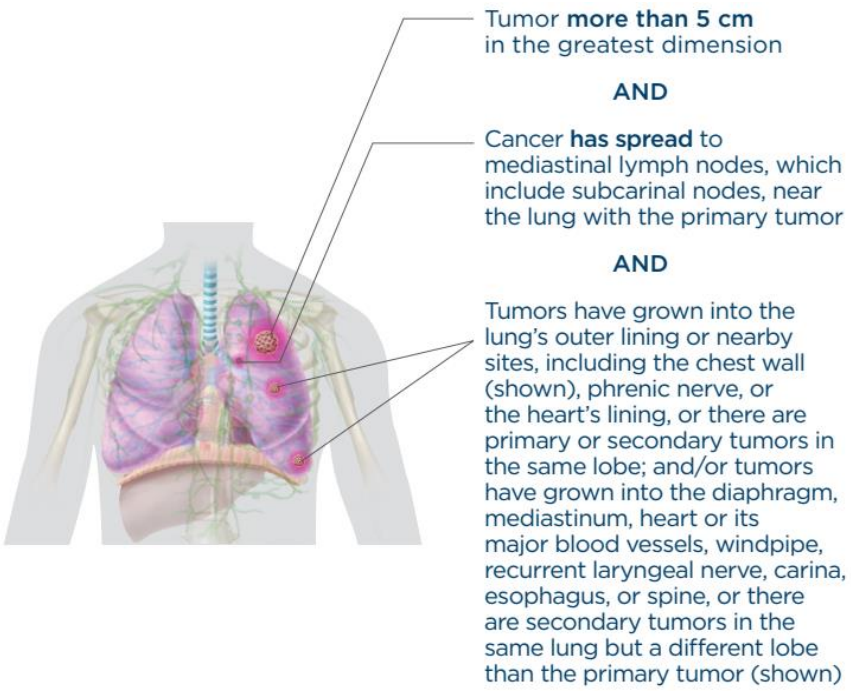

Figure 2.2: Example of stage IIIB NSCLC with a tumor bigger than 5 cm in greatest dimension, spread to mediastinal lymph nodes, and tumors growing into the lung's outer lining (or other tumor growths described in the figure) [17].

The other combinations of tumor size and spread are shown in table 1, and the abbreviations have their explanations in appendix A. Every patient gets this kind of classification for their cancer, and further treatment depends on this.

2.2.4 Survival and treatment

The newest report of cancer in Norway in 2021 by the cancer registry of Norway, shows that there has been a slight increase in the five-year relative survival for lung cancer [20]. Compared to the previous five-year period, the percentage of survival five years after diagnosis has increased from 19.3% to 25.7% for males and 26.2% to 32.8% for females, in the period of 2017-2021. This five-year survival rate depends on the stage of the lung cancer, and varies from 70,8% for stage I to only 22,9% for stage III [3].

We have different methods to treat cancer, and the most common methods are surgery, chemotherapy, and radiotherapy. Surgery or radiotherapy can cure stage I-III NSCLC, and surgery should be recommended as early as possible to patients with resectable cancer [3]. For patients in this staging group that have unresectable cancer, radiotherapy is an alternative. In general, chemotherapy is not a curative treatment but can increase the chance of cure together with surgery and/or radiotherapy. Immunotherapy is also an additional treatment method in

combination with chemoradiotherapy that can be offered for selected patients as a result from the PACIFIC study [21]. The overall survival median increased from 29.1 to 47.5 months from treatment with durvalumab.

Some patients with LA-NSCLC may consider surgery, but surgery alone will only cure a few patients [2]. Suitable patients with LA-NSCLC should be offered a combination of chemotherapy and radiotherapy. Radiotherapy should be offered alone for patients that are not candidates for the combination treatment. Radiotherapy is the treatment method of LA-NSCLC that this thesis will focus on, but the patients introduced might have received other treatment methods as well.

2.3 Radiotherapy

Radiotherapy can cause damage to the cancer without opening the patient's body and leaving scars. It is also a good alternative for cancer forms that are hard to reach with surgery, and it often achieves reasonable probability of tumor control [22]. This is especially for long-term control of tumors of lung, cervix, bladder, prostate, skin, head, and neck.

There are two main types of radiotherapy, external beam and internal. The treatment choice depends on multiple factors like: type of cancer, tumor location and size, and how close the tumor is to radiation sensitive tissue [23]. External beam radiotherapy aims radiation towards the tumor from a machine outside the body, and the machine can rotate to irradiate from many angles. For internal radiation therapy, the radiation source is placed inside the body, near the tumor. The radiotherapy treatment of LA-NSCLC consists of external beam treatment which will be the main focus in this thesis.

Cancer treatment typically aims at damaging the DNA structure of the cancerous cells. The damage will hopefully stop these tumor cells from replicating, slow it down, or kill them. To cause this damage radiotherapy uses ionizing radiation delivered at high energies. Photons, electrons, protons, and other particles like carbon ions can be used. This thesis is further based on radiotherapy with photons that is the state-of-the-art for treatment of LA-NSCLC. Proton treatment of lung cancer has no evidence of increased survival, better local control, or less side effects, compared to radiotherapy of photons [3].

Absorbed dose is an important quantity in radiotherapy and is defined as the mean energy imparted in mass by the ionizing radiation [24]. The unit is gray (Gy), where 1 Gy = 1 Joule per kilogram (J/kg). Radiotherapy of 60-66 Gy is in general recommended for patients with LA-NSCLC [2]. More of the physics behind radiotherapy with photons and how it results in DNA damage is represented in the paragraphs below.

2.3.1 Photon interactions with matter

In radiotherapy a beam of x-ray photons can be aimed towards the body from the outside, directed towards the tumor. Even though photons are the radiation modality, it is the charged particles, produced inside the body by the photon beam, that causes the cell killing or damage to the DNA [24]. These particles produced in matter are often denoted as secondary particles. Photons are thereby termed indirectly ionizing, while the secondary radiation of charged particles is the ionizing radiation. These secondary particles are usually electrons, and they deposit their energy close to the interaction site where they were produced. Secondary photons may also be created and will contribute to the photon intensity and can also further produce more secondary electrons.

The photons are either transmitted through the matter or attenuated, and there are different factors affecting where the energy of the beam will be deposited. The intensity *I(x)* of a narrow monoenergetic photon beam, attenuated by a material with thickness *x*, is given by equation (2.1) [15]. The beam intensity depends on the original intensity of the unattenuated beam (*I(0)*), the linear attenuation coefficient ($\mu(hv, Z)$), which depends on the photon energy hv and the atomic number *Z* of the attenuator.

$$I(x) = I(0)e^{-\mu(hv,Z)x}. \tag{2.1}$$

The linear attenuation coefficient increases with the atomic number and density of the attenuator, and decreases with the energy of the x-ray photons [25].

The photon can be attenuated and deposit its energy differently, by different interactions with the atoms of the attenuator. Which type of interaction the photon will undergo, depends on its energy *hv* and the attenuators atomic number *Z*. The three main forms of photon interactions are: *photoelectric effect*, *Compton effect*, and *pair production*. We can divide the three interactions in regions of relative predominance, represented in figure 2.3 [15]. Photons interact with soft tissue (low atomic numbers) predominantly by the Compton effect. The photon energies used in radiotherapy are typically around 6-15 MeV.

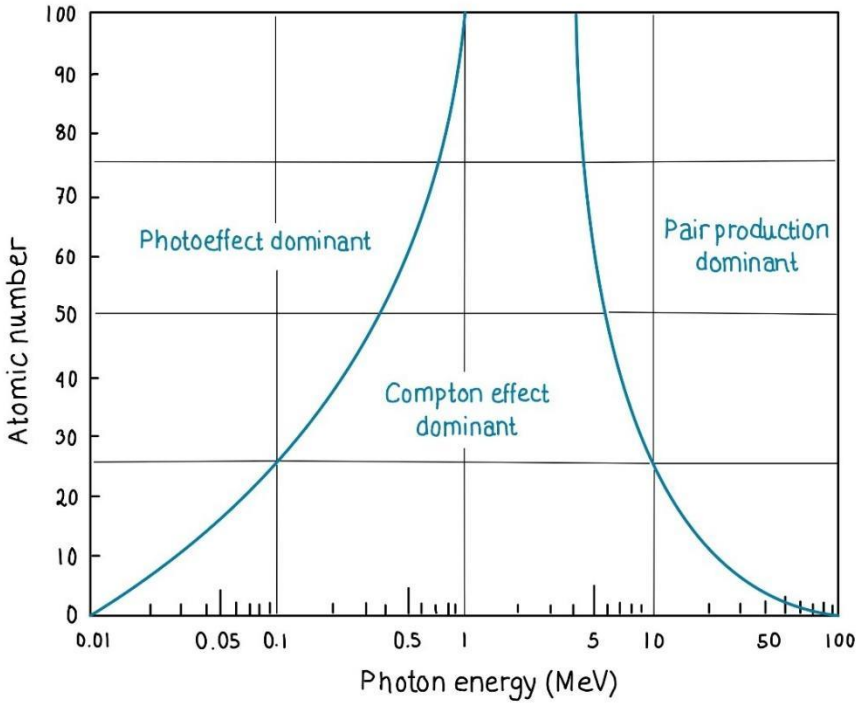

Figure 2.3: Relative predominance for different photon interactions (Photoelectric effect, Compton effect, and pair production) in matter of different atomic numbers, depending on photon energy (MeV). Figure inspired from [15]. A 10 MeV photon will interact with lead predominantly through pair production, but interaction with tissue predominantly by Compton scattering.

Compton effect occurs when a photon, with energy *hv*, collides with a loosely bound atomic electron, and the electron gets kicked out of the atom [24]. The incident photon loses some of its energy to the electron that gets kicked out. The scattered photon travels in a different angle than the recoil electron after the collision. The interaction is illustrated in figure 2.4.

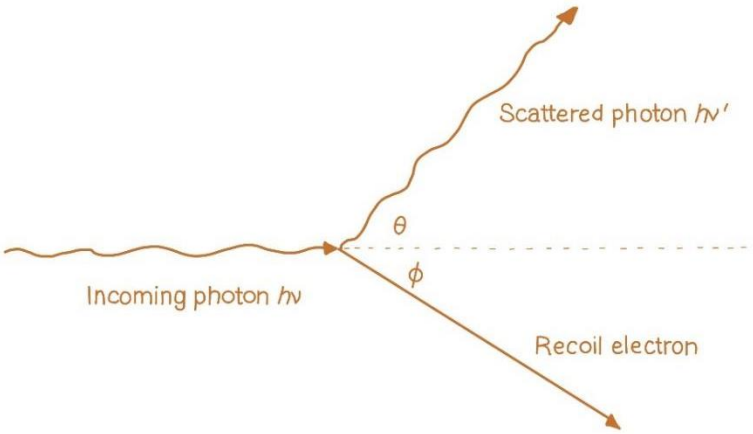

Figure 2.4: Compton scattering, with scattering angles and energies. Figure inspired from [24].

Compton effect is the most dominant interaction for photons of radiotherapy, but the two other interactions will be explained briefly. Photoelectric effect occurs when an incoming photon transfers all its energy to a *photoelectron* (an orbital electron of the absorber atom), which gets ejected with all the photon energy except the binding energy of the electron [25]. The vacancy from the ejected electron then gets filled by an electron from the upper energy shell, and this process results in emission of a characteristic x-ray or Auger electron. The photoelectric effect is illustrated in figure 2.5.

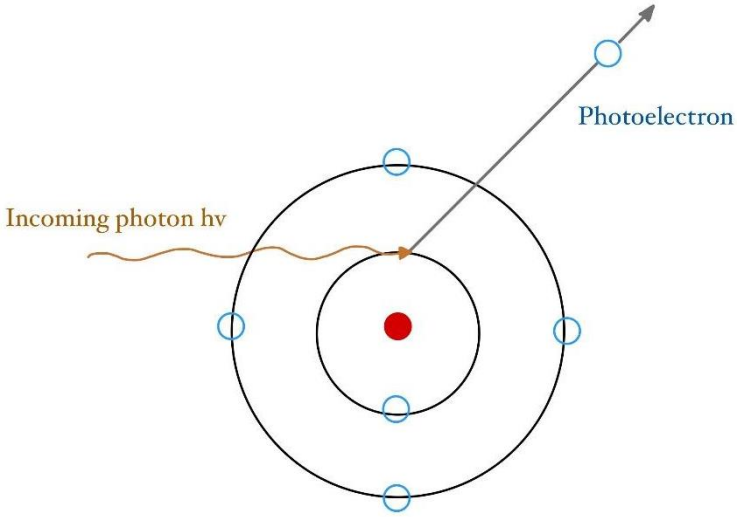

Figure 2.5: Illustration of the photoelectric effect inspired from [24]. Incoming photon is absorbed by the atom, and ejects a photoelectron.

For pair production presented in figure 2.6, the photon is absorbed in the electric field of the nucleus, resulting in creation of an electron-positron pair that is being emitted [24]. Energy is conserved in the process and the incoming photon needs energy greater than 1.02 MeV to interact with the nucleus.

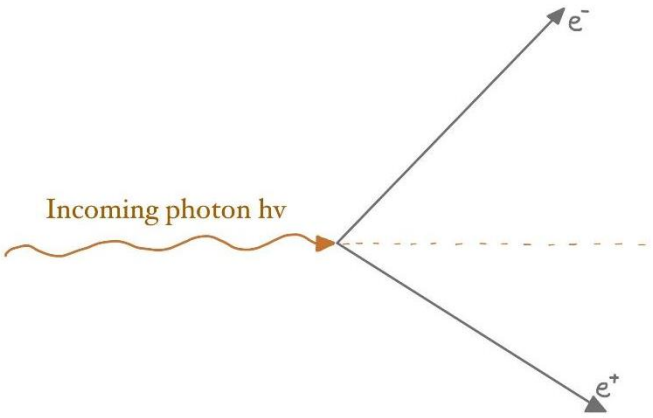

Figure 2.6: Illustration of pair production inspired from [24]. Incoming photon that results in emission of an electron-positron pair.

2.3.2 LINAC

A linear accelerator (LINAC) is a device used in radiotherapy to create the x-ray photons that will target the tumor. The LINAC uses high-frequency electromagnetic waves to accelerate charged electrons, so that they have enough energy to produce the x-ray photons when they strike a certain target. The major components in a typical LINAC are a *power supply*, *modulator*, *magnetron* (or *klystron*), *electron gun*, and an *accelerator tube/structure*. All components are represented in figure 2.7.

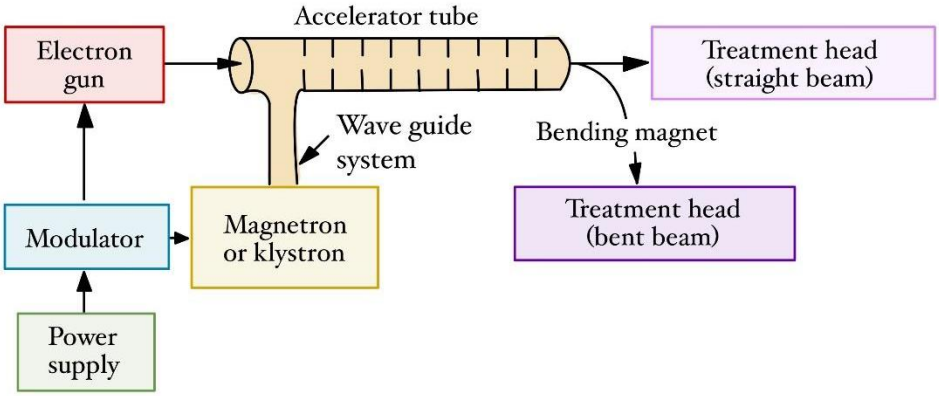

Figure 2.7: Components of a typical linear accelerator (Power supply, modulator, magnetron/klystron, electron gun, accelerator tube, and two possible treatment heads) represented in a block diagram. Figure inspired by [26].

The power supply makes a direct current power which the modulator receives and turns into high voltage pulses with duration of a few microseconds. The magnetron receives these pulses simultaneously as the electron gun. Electrons are produced in the electron gun and are in pulses injected to the accelerator tube. The magnetron produces pulsed microwaves and transfers them to the accelerator tube. The way these electrons and microwaves have a special timing of release, makes the electrons gain energy on their way to the target material for x-ray production. [26]

There are different types of LINAC for clinical use, with different megavoltage ranges for the x-ray production. Some produce 4 or 6 MV (low range), but a typical modern LINAC with high energy produces photon energies at 6 and 18 MV [15]. The electron beam can either travel straight to the treatment head or be bent with a bending magnet, as shown in figure 2.7. For low energy LINACs with a standing waveguide/accelerator tube, the electron beam travels straight down parallel to the radiation beam. It would be ideal if every tube could be mounted parallel like this, but the length of high energy LINACs makes it difficult to achieve, so the electron beam must be bent [24]. LINACs can also use electrons instead of photons, as radiation source when treating shallow cancer.

2.3.3 Radiobiology

There are two ways the direct ionizing radiation can damage the cell when it is absorbed in the biological material: direct and indirect action [15]. Direct action interacts directly with the target within the cell. The atoms of the target may then be ionized or excited through Coulomb interactions, leading to biological damage eventually. Indirect action does not interact directly with the target, but through other atoms of the cell to produce free radicals. Typically, this will be water since the cells are mainly made up of water. Irradiation of water can, through the steps of equation (2.2) and (2.3), produce a highly reactive hydroxyl radical OH• [16].

$$H_2O \rightarrow H_2O^+ + e^- \tag{2.2}$$

$$H_2O^+ + H_2O \rightarrow H_3O^+ + OH\bullet \tag{2.3}$$

The free radicals can produce chemical changes in the target leading to biological damage, because they have a valence electron that is unpaired. If we study x-ray radiation, about two-third of biological damage is caused by indirect action like this [15]. The steps producing the biological damage are then summed up to: a) photon interaction produces an electron, b) the electron produces free radicals, c) the free radical damages the target/DNA.

The DNA is a large molecule with a helical structure and has two strands held together by hydrogen bonds [16]. To damage the DNA in the cancerous cells with radiotherapy, there need to be enough breaks of the DNA strands. If the radiation only breaks one of the strands (single-strand break), the DNA can repair itself by copying the opposite strand. If both strands are damaged (double-strand break), the DNA will not repair itself easily and it depends on the distance between the damage. Single-strand break, double-strand break separated enough to repair, and double-strand break too close to repair, are illustrated in figure 2.8 [25]. The damage caused immediately after 1 Gy of x-ray is approximately 40 double-strand breaks and 1000 single-strand breaks per cell [16].

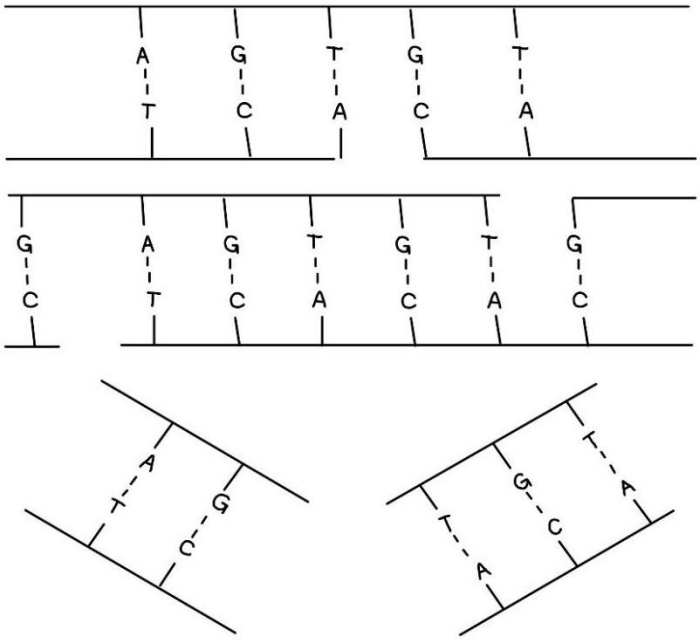

Figure 2.8: Different breakage of DNA bonds. Single-strand break (at the top), double-strand break separated enough to repair (in the middle), and double-strand break too close to repair (at the bottom). Illustrations inspired by [25].

If a double strand break happens to non-malignant cells and they don't repair themselves, it can induce apoptotic cell death [27]. This is a mechanism for the cells to be programmed to die when something abnormal (some kind of stimuli) happens to them [28]. The cell cycle consists of replicating its DNA (synthesis) and separating the chromosomes and splitting them into two new similar cells (mitosis). How radiosensitive the cell is, depends on when in this cycle the irradiation occurs, and it is most sensitive at or close to mitosis [16]. The 5 R's of radiotherapy represents biological factors for cell survival: *radiosensitivity*, *repair*, *repopulation*, *redistribution,* and *reoxygenation* [15]. Cells have different radiosensitivity, cells can repair radiation damage, and cells repopulate even though it receives radiation. Redistribution in cell population throughout the cell cycle phases and reoxygenation of hypoxic cells, both makes them more radiosensitive for a new dose of radiation.

2.3.4 Treatment response and side effects

High enough energies are needed so that the cancerous cells don't repair themselves, but at the same time normal tissue must be spared. Damaging normal cells can cause different negative effects for the patient. Fortunately, normal cells are repairing themselves more easily than cancer cells do.

There is a difference between tumor control and normal tissue toxicity that is called the therapeutic ratio [29]. The therapeutic window, closely connected to the therapeutic ratio, is a figurative space between treatment failure and toxicity [29]. The larger the therapeutic window is, the safer and more effective treatment. The therapeutic window can be seen as the area between curve A and curve B in figure 2.9, where curve A represents the tumor control probability (TCP) and curve B the normal tissue complication probability (NTCP) [15]. Both TCP and NTCP are varying with dose, where the therapeutic ratio is the measure of the difference between them, while the therapeutic window is a conceptual area between the two curves.

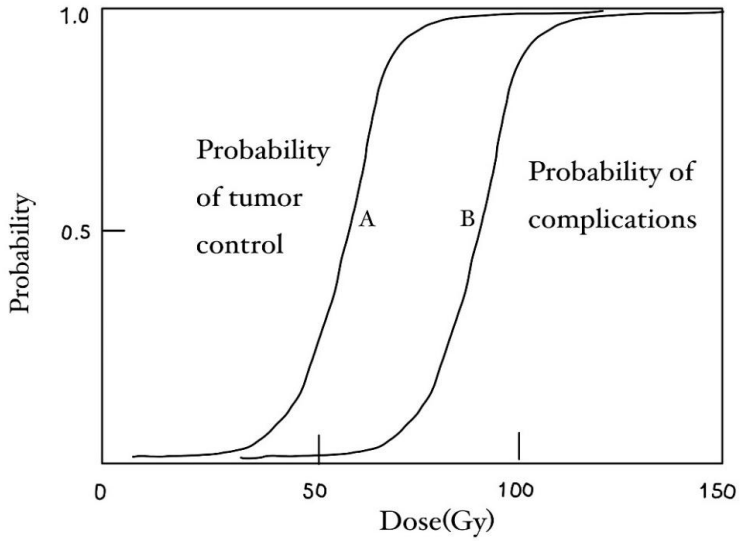

Figure 2.9: Therapeutic ratio and therapeutic window. Curve A as TCP and curve B as NTCP. Figure inspired by [15].

Some organs surrounding the tumor during radiotherapy are also exposed for radiation and need to be considered when talking about complications like NTCP. The organs that are especially concerned are referred to as organs at risk (OAR). For stage III LA-NSCLC these organs are heart, esophagus, spinal canal and both of the lungs. In patients with cranial tumors, the brachial plexus is also an important OAR. For lungs, acute effects like radiation-induced pneumonitis can emerge 1-8 months after radiation treatment [2]. The late effects of the lungs, like radiation-induced fibrosis, do not occur until 6 months after treatment. In some cases, patients can get problems and/or pain with swallowing under and after the treatment, because of radiation to esophagus [2]. So, there can be big and small side effects when irradiating the thorax region.

Earlier, radiation-induced heart toxicity was rarely reported as a side effect, and that the patients almost never lived long enough to develop such side effects affecting the heart [2]. On the other hand, increased reporting of such side effects was expected in line with increased survival and more effective radiotherapy. So, dose limits and recommendations are important, like how the volume of the heart that receives high doses (> 35-40 Gy) needs to be as small as possible without jeopardizing bad coverage of the tumor. Now, a study by McWilliam et al. resulted in a significant association between dose to heart region and overall survival [30].

Fractionation

The total dose prescribed for the patient's treatment cannot be given all at once, because it would damage the patient's normal-tissue, and in the worst case kill the patient. To treat cancer with radiotherapy, the prescribed dose needs to be given in fractions over multiple weeks. The therapeutic ratio and therapeutic window can be improved by fractionation, but this has not always been the recommended practice. In 1904, Perthes recommended radiation treatment of one session, called expedited or massive-dose treatment [31]. It led to unexpected toxic reactions and resulted in a growing awareness of how time during dose delivery could influence the biological effects. Several approaches for fractionation have been researched since.

During the 1980s there was a further major development in radiobiology of normal tissue, when it was realized that normal-tissue responses are affected by change in dose fractionation [22]. In an attempt to improve the therapeutic ratio there were small clinical tests with few patients, and resulted in two new approaches to fractionation: accelerated fractionation and hyperfractionation [31]. Today, standard fractionation treatment is given once daily, 5 days per week, and no more than 2 Gy per fraction [29]. The accelerated fractionation gives over 10 Gy

per week. Hyperfractionation schemes have more than one fraction per day but decrease the fraction size. Hypofractionation is a method that increases fraction size with or without decreasing the number of fractions per week. The choice of fractionation scheme depends on the patient's general health situation and life expectancy [3]. For LA-NSCLC patients, like the ones studied in this thesis, standard fractionation with 2 Gy per fraction is most common. Palliative patients with short life expectancy could get hypofractionation with 8 Gy per day for an example [3], and other cancer types may benefit from other fractionation methods than the standard method.

2.3.5 Standard radiotherapy workflow and treatment planning

The workflow of radiotherapy starts after the patient is diagnosed and radiotherapy is chosen as the suitable treatment method. There are multiple ways to deliver radiotherapy. Before the planning phase starts the patient needs to be imaged so that different important volumes can be defined and delineated. When the contouring of volumes is done and a treatment plan is made, the plan needs to be evaluated and approved. Finally, quality assurance (QA) is needed before the patient can start the fractionated treatment delivery. The whole workflow is illustrated in figure 2.10.

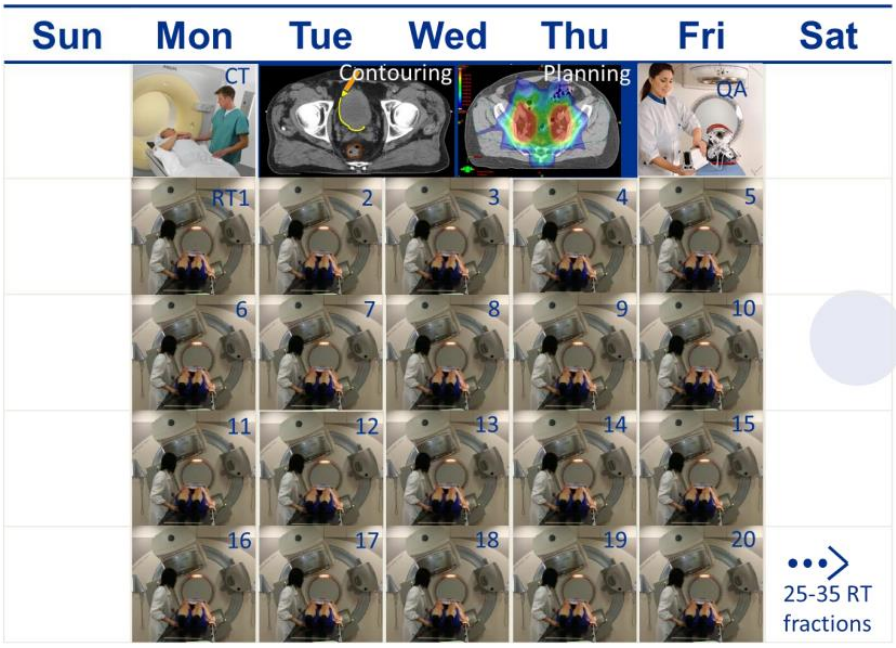

Figure 2.10: Radiotherapy workflow. Figure from Liv Hysing.

Imaging

To be able to deliver the dose correctly, imaging is a crucial part of the workflow. Image guidance is not only important in diagnosis and as the first step of the workflow, but also later for patient setup, tumor localization and motion monitoring, treatment response and evaluation [32]. So, most of the advances in radiation oncology over the last three decades, is owing to the headway in medical imaging techniques like CT, magnetic resonance imaging (MRI), PET, and single photon emission computed tomography (SPECT).

CT has been a standard imaging technique used for treatment planning and dose calculation, for several decades [33]. This technique is used to get high dosimetric accuracy and estimates linear attenuation coefficients for x-rays. The CT scans consist of pixel information expressed in Hounsfield Units (HU), where some value is set for air and a value of zero is represented as water [24]. The CT scanner is calibrated to measure the relationship between the HU and tissue density. This makes it possible to later calculate the dose deposition that depends on tissue density.

As figure 2.10 shows, CT scans are a typical part of the workflow before the treatment delivery can be planned. CT, as well as MRI, makes it possible to reconstruct three-dimensional (3D) shapes of the body and treatment area [32]. Thereby, delineating can be done with great precision, which reduces the chance of missing the tumor and minimizes exposure of normal tissue. Also, four-dimensional (4DCT) can be made by acquiring repeated CT scans over a short period of time, and 4DCT will be explained further later on. Image guidance for patient setup ensures that the patient is located in the same position as for the planning image. This increases the chance of correct dose distribution. There exists different fixation equipment as aid to achieve correct positioning, repetitively throughout the whole treatment period.

Contouring: volume delineation

The aim of curative radiotherapy is decreasing tumor cells to an amount that achieves permanent tumor control, and the volumes irradiated have to include tumor and some expected subclinical spread area [34]. The different volumes often need different dose levels of irradiation. The prior volumes that should be defined in the planning phase are Gross Tumor Volume (GTV) and Clinical Target Volume (CTV). The GTV is the visible extent and location of malignant growth, but the CTV includes GTV with an additional margin for microscopic extension of primary tumor or regional lymph node spread [24].

GTV delineation of the primary tumor and GTV of lymph nodes should be drawn separately if it is possible to distinguish them [35]. For patients with 4DCT scans, an internal gross tumor volume (iGTV) can be defined as GTV including motion of the tumor from all the phases of the 4DCT [36]. Similarly, the motion of CTV, sometimes are delineated as the internal clinical target volume (iCTV). In figure 2.11 GTV, iGTV and CTV are represented, surrounded by the planning target volume (PTV). PTV takes patient movements and setup errors into account and ensures that requested dose is delivered to the CTV with clinical acceptable probability [2].

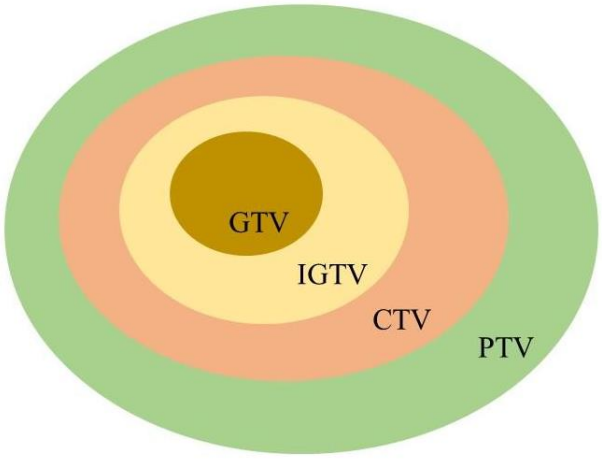

Figure 2.11: Different volumes that need to be delineated for each patient: GTV, IGTV, CTV and PTV. Irradiation is planned for the whole PTV. Inspired by [2].

In addition to the target that should be irradiated, it also needs to delineate some parts of the body that we need to spare for radiation. The treatment plan can be influenced by the presence of OAR because of its radiation sensitivity [34]. OAR could also have possible movement during the treatment and uncertainties by setup errors, and this must be considered during the treatment planning and treatment course.

Treatment planning and techniques

A dosimetrist uses the CT scans in a treatment planning system to create the treatment plan. An important step in the planning phase is to select which radiotherapeutic technique the patient should receive. Beam energy, field size and beam direction are different factors that need to be considered when constructing a treatment plan. Multi-leaf collimators (MLC) allow flexible adjustment of the fields of radiation, adjusting the fields towards the tumor shape and OAR [37].

In many years, 3D conformal radiotherapy has been the standard technique, with a goal of achieving a high dose which conforms to the PTV but also spares the OARs for high doses [24]. Conforming the dose to the PTV involves shaping the radiation field to the beam's eye-view of the PTV. This had earlier been done with metal blocks, but the MLC technique gives fast automatic verifiable beam shaping. Until 2019 and the pulmDIBH study, 3D conformal radiotherapy was the treatment technique of LA-NSCLC at HUH. Now, intensity-modulated radiotherapy (IMRT) has been widely adopted for treatment of lung cancer [38], and is the state-of-the-art treatment technique for this cancer form. Most of the patients studied in this thesis received IMRT.

IMRT is usually based on inverse planning, where the dose-volume restrictions for the target volume and normal tissue are defined and then the treatment plan is optimized by a computer algorithm [39]. The system tries to find the optimal dose distribution by step-by-step minimizing the distance between the calculated dose distribution and the pre-set dose-volume restrictions [40]. Inverse treatment planning usually results in an ideal photon-fluence distribution for each selected beam angle [37]. IMRT generally leads to non-uniform dose distributions to organs and normal tissue [22].

IMRT can be delivered with MLC in two main methods: "step-and-shoot" approach and "dynamic" dose delivery concept [37]. The inverse planning produces an "ideal" fluence map for every beam direction, and for the "step-and-shoot" approach each segment of the map has its own shape and number of monitor units (MU) for delivery. The beam irradiates the MU matched to the segment, then the MLC moves to the next segment while the beam is turned off. The "dynamic" MLC technique is obtained by various velocities of the moving leaves, while the treatment beam is not switched off during the movements.

Volumetric modulated arc therapy (VMAT) is a developed delivery technique extended from IMRT, where an optimized 3D dose distribution can be delivered in a single gantry rotation [41]. VMAT uses the dynamic MLC technique as described above and each rotation of the LINAC around the patient is called an arc.

Plan evaluation

A dosimetrist can conclude that there is no need for further optimization of the plan, and then the responsible oncologist will evaluate the plan together with the dosimetrist. The plan evaluation mostly consists of studying the dose distribution. It needs to be evaluated if the target cover is satisfying, and that the OARs receive doses below constraints. PTV coverage should be between 95-107% of the prescribed dose, by recommendations from The International Commission of Radiation Units and Measurements (ICRU) [42]. The dose distribution is represented in a 3D configuration of the body (with structures delineated) and can be studied from different angles. Figure 2.12 represents a transversal and frontal view of a treatment plan, with a dose color wash distribution. The treatment fields are also present, as well as the PTV delineated in red, and CTV delineated in pink inside of the PTV.

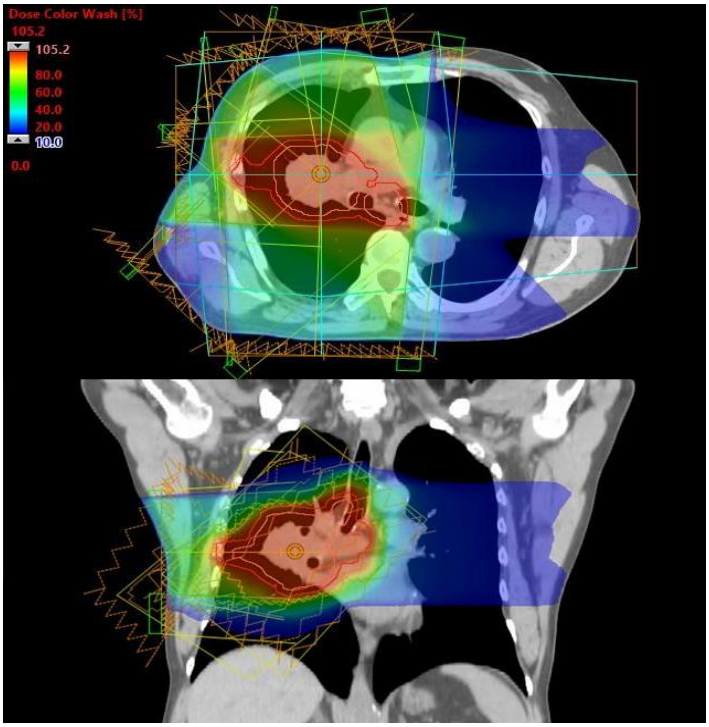

Figure 2.12: Dose color wash distribution of a treatment plan for a patient with LA-NSCLC, represented by a transversal view (top) and frontal view (bottom). Treatment fields represented surrounding the patient. PTV delineated in red, and CTV delineated in pink.

Dose volume histograms (DVH) is a graphical representation of radiation distribution within a defined volume and makes it easier to summarize and analyze the 3D data [24]. Figure 2.13 is an example of a DVH with different structure volumes from a patient with LA-NSCLC. Here, dose distributions of different organs can be studied more closely. Vertically there will be an axis for percentage of structure volume, and doses in Gy and relative dose [%] is represented

in the horizontal axis. Naturally 100% volume of a structure will receive 0 or more Gy, but only 20% of the heart's volume (yellow line in figure 2.13) will receive a dose equal or higher than 26,4 Gy. An example of a simple and logical analysis of this DVH is that the higher dose, the smaller volume of the heart receives this amount of dose. PTV (red line in figure 2.13) should have higher doses for the whole volume as the figure shows, since that's the volume we are targeting.

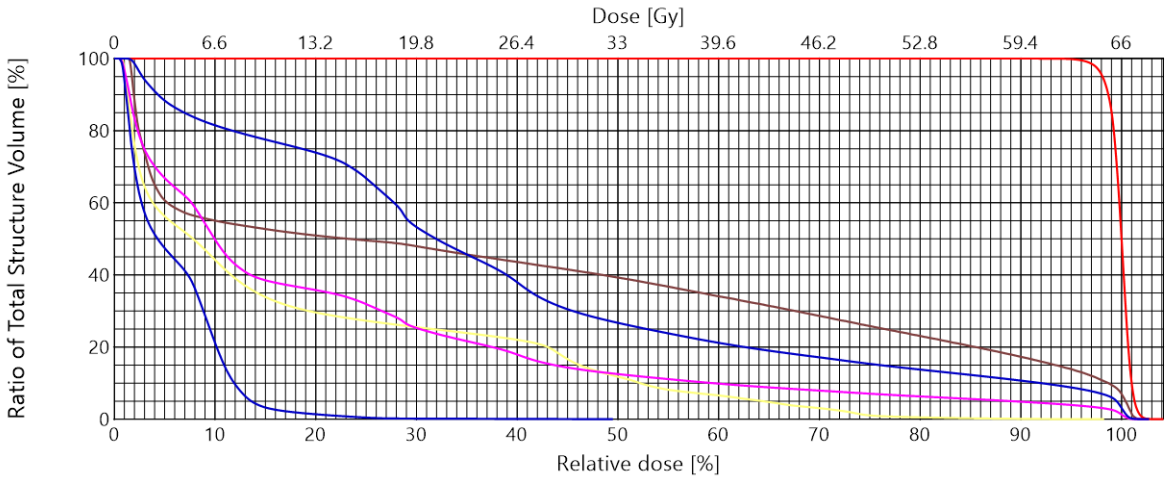

Figure 2.13: DVH of patient number 24, with following volumes represented: red (PTV), bottom blue (left lung), top blue (right lung), pink (both lungs), yellow (heart), and brown (esophagus). Relative dose [%] and total dose [Gy] horizontally, and structure volume [%] vertically on the histogram.

In this way, the dose to an OAR (like the lungs) can be studied separately, and the oncologist and dosimetrist can decide if it needs a lower dose. Dose limit decisions are made based on recommendations from the Norwegian Radiation and Nuclear Safety Authority (DSA) and ICRU. One of the recommendations is that the mean lung dose is supposed to be less than 20 Gy for conventional fractionation [2]. Mean dose of a certain structure comes from summing the doses in each voxel of that structure in the CT scan and dividing it by the total number of voxels.

Another way of collecting dose statistics for a given structure is finding a volume, V_{Dref}, corresponding to a reference dose, D_{ref} [24]. This is the sum of all voxels receiving a dose greater than or equal to the reference dose. D_{ref} can be expressed as prescribed dose or some dose in Gy, or percentage of prescribed dose. A dose D_{Vref}, corresponding to a volume equal to V_{ref} can also be found. The treatment plan can be evaluated based on dose statistic parameters like this, and they can be found by the DVHs. Changing the plan to decrease an OAR dose,

may result in a poorer dose cover of the tumor. The DVHs can then be used to compare different treatment plans in the evaluation, by studying these kinds of parameters.

Quality assurance

Procedures to ensure consistency of the medical prescription and safe delivery of that prescription is necessary, and this is referred to as QA [15]. This concerns all the aspects of the treatment process and should be implemented for all staff, cooperatively. Minimal dose to normal tissue, minimal exposure of employers, sufficient dose to the target volume, are some of the aspects of the quality assurance.

Annual, monthly, and daily test that ensures that the LINAC delivers the prescribed dose correctly, and the test results are either within a tolerance level or unacceptable. Daily QA has a machine-type tolerance of 3% for x-ray output constancy and 2 mm for laser localization and distance indicator, for IMRT [43]. The monthly QA is more advanced and consists of more mechanical tests and gating functionality. The same goes for the annual QA, with increase of dosimetry procedures.

Treatment delivery

Image guided radiotherapy (IGRT) is a technique that can be implemented right before the patient receives its fraction. As mentioned, image guidance ensures that the relative position of the target volume is as close to the treatment plan as possible. IGRT may reduce treatment margins, and also reduce the chance of complications and target miss [15]. Cone-beam computed tomography (CBCT) is a CT machine shaped as a cone beam. This can be a part of the LINAC, and when the patients are ready for delivery of the treatment fraction, a CBCT can be taken while they lie on the treatment table [15]. The CBCT is then compared to the planning CT (pCT), and then it can be decided if the patient position needs fine tuning.

Bones are the easiest to use as guidance for comparison of the scans. Implementing markers in the patient's body can also be helpful for position adjusting based on soft-tissue target volumes [24]. In clinical practice, IGRT and usage of CBCT for each fraction can also make us aware of anatomical changes during the treatment course. Some anatomical changes can be critical for the treatment result, and it is important to develop systems for detecting and handling this. If anatomical changes occur, the plan can be adjusted by adaptive ART to get the best treatment possible. ART will be described in more detail below.

2.4 Radiotherapy of LA-NSCLC

2.4.1 Breathing motion and anatomical changes in the thorax region

Naturally, the chest area moves because of our breathing and is thereby a challenging region to treat with radiotherapy. The tumor could move when breathing and there then is a risk of irradiating healthy tissue instead. The movement of the MLC leaves in IMRT together with respiratory-induced tumor motion can cause this unwanted motion artifact in dose delivery, which we call interplay effect [44].

To account for internal motion, 4DCT scans should be used in treatment planning of lung cancer when treatment is delivered in free breathing [36]. This includes a set of 3DCT scans of the patient during a free breathing session, to make a set of CT scans of different phases of the patient's respiration cycle. From this, an average intensity projection (AIP) can be reconstructed as an average of all breathing phases. 4DCT gives a full range of possible positions of the tumor and critical organs, and the motion uncertainties can then be implemented in the contouring, treatment plan and evaluation [45].

In addition, there are some typical anatomical changes that can occur during the whole treatment, over days or weeks. Kwint et al. [46] did a study about intra thoracic anatomical changes (ITACs) during radiotherapy of patients with lung cancer. Of 177 lung cancer patients in the study, there were observed ITACs in 72% of the patients during their course of radiotherapy. Of all observed ITACs, 35% were tumor regression, 27% had tumor baseline shift, 19% changes in atelectasis, 10% tumor progression, 6% pleural effusion and 3% infiltrative changes.

Atelectasis is described as a state of a non-aerated and collapsed region of the lung [47]. This condition is usually associated with chest or lung disorders. It comes from an underlying disease and is not a disease itself. Pleural effusion is an accumulation of fluid in the pleural space, between the lungs and the chest cavity [48]. It can be discovered in x-ray and CT images of the chest. Tumor regression means that the size of the tumor is smaller, and with tumor progression it is getting bigger. The goal of radiotherapy, and other treatment methods, is usually to shrink the tumor. Naturally, tumor regression as an anatomical change during the

treatment course is normal. A baseline shift of the tumor can also be quite common and can also be a result of other anatomical changes. Infiltrative changes of the lungs are not that common, but blood or other substances in the lung may cause this.

Both interplay and ITACs can affect the treatment, and there are different ways to take this into account. ITACs can be monitored by ART and traffic light protocols, which will be studied more later in this thesis. Interplay effects can be reduced by different treatment techniques based on how big the breathing pattern uncertainties are for the patient, like deep inspiration breath hold (DIBH) and gating.

2.4.2 DIBH treatment and gating techniques

A reliable estimation of the tumor position is important in radiotherapy, but can sometimes be difficult in treatment of the thoracic cavity because of motion. 4DCT and volume delineation will help to improve tumor coverage for patients with NSCLC. If the patient's respiratory motion is regular, the patients can get a “free-breathing” treatment, where they can breathe normally during the treatment delivery [36]. The treatment plan is then made from the 4DCT scans. For patients with irregular respiratory motion, DIBH technique or respiratory gating can be considered as respiratory management. The DIBH technique involves the patient holding their breath for approximately 20 seconds, while a CT scan is being carried out by the radiation therapist. The treatment plan can then be made from this scan, and delivery is given with the same DIBH position of the patient.

Gating techniques reduce the target motion during treatment because the irradiation is limited to a certain respiratory phase [49]. The first respiratory gating technique was developed in 1990, and during the early 2000s it was improved to a real time monitoring free-breathing system. Multiple breathing synchronized radiotherapy (BSRT) systems have been developed, and there are different organ motion detectors [50]. A voltage signal is derived from the organ displacement detector in BSRT, and when the signal falls between a certain level it produces a gate pulse that authorizes the treatment machine. Video camera systems to monitor markers placed on the patient’s chest, or spirometer for monitoring volume of air in the lungs, are two examples of detector systems. A reported gating system uses multiple fluoroscopic units as x-ray detectors to make continuous imaging of implanted gold markers in the tumor, and when the markers are located within a preassigned region the beam delivery starts. This method gates

the delivery from the LINAC, so that the delivery stops when the target volume is out of sight and then spares normal tissue.

2.4.3 Adaptive radiation treatment

Anatomical changes between each fraction, like intra-fractional tumor motion and intra-fractional anatomic changes, affects the accuracy of the treatment [45]. Reducing these uncertainties improves the therapeutic ratio, and studies suggest that image guidance and motion management can improve local control and overall survival for NSCLC patients.

Large changes in lung tissue cannot always be handled by set margins when treatment planning, but it requires a more individualized adaptive strategy [51]. Atelectasis and pleural effusion, as described earlier, are anatomical changes that impact the geometry of the treatment target and normal tissue. This can impact the dosimetry, and ART is a process using systematic feedback of measurements to modify the treatment plan if needed [52]. ART also needs a controller to manage the whole process and make decisions for when adaptive modifications are needed.

ART can be implemented off-line between fractions or on-line immediately prior to a fraction [53]. Off-line ART has the advantage that conventional CT or MRI can be used for replanning, as it has better imaging quality than the in-room imaging. On the other hand, off-line ART may not keep up with anatomical changes between each fraction and is not capable of responding rapidly enough to these kinds of changes. On-line ART has this advantage, but the whole process is supposed to take place while the patient stays in the same position on the treatment table, which can be a time challenge. Changes like bladder filling can also take place between the in-room imaging and the treatment delivery, during the evaluation and re-optimization with on-line ART. The Ethos ART machine is dedicated for on-line ART, but at HUH it is currently only available for radiation therapy of the pelvic.

Which and how often adaptations are needed depends on the treatment location, and treatment of thorax and/or abdominal locations like lung cancer have a bigger expectancy of anatomical shifts in OARs. The ART process can be triggered at some frequency, e.g daily for on-line ART and weekly for off-line ART [53]. Some changes in OARs that can impact the location or overlap with the treatment target, may be predictable. If so, the initial simulation process could include simulations where these predicted changes are considered. A plan library of different plans, for each possible outcome, can be made and used as an on-line ART method.

Based on the CBCT taken in advance of the fraction, a decision is made of which plan is most suitable for the patient that day. The decision is made while the patient lies on the table, and the treatment is delivered immediately after. An ART method for lung cancer patients needs to be triggered by anatomical changes, which can be quite individual for each patient. A traffic light protocol can be a solution for these patients.

Traffic light protocol

The traffic light protocol is an off-line type of adaptation and is the main focus of this thesis. The traffic light protocol developed by Kwint et al. [46] is used as an implement for determining whether the treatment needs adaptation. A radiation therapy technologist (RTT) studies the patient's daily CBCT scan, that is taken the moment before each fraction of the treatment. The RTT then decides a suitable traffic light color for this CBCT scan, based on requirements and guidelines from the protocol. The color evaluation is based on how well the treatment plan is suitable for the patient's current anatomy that day. When comparing the CBCT to the planning CT, it can be evaluated if there are any anatomical changes present, and a color is given based on the extent. The color categories are red, orange, yellow or green. Red represents big anatomical changes, and the plan requires adaptation before the patient can continue the treatment. Orange means the anatomical changes are noteworthy and the dosimetric impact needs an evaluation by a medical physicist and oncologist while the treatment is given. A new CT can be ordered and replan is made if it is needed for future fractions. Yellow is given if there are smaller changes that are expected to have low impact and the treatment will still have good target cover, and the changes are noted. Green means small or no changes at all, so there is no need for adaptations and the treatment can continue as planned.

The anatomical changes are registered with a code that represents what type of change that patient has according to the CBCT scan that day. The amount and type of change can differ throughout the whole treatment and registering this in addition to the color is done for each fraction. Changes like atelectasis, pleural effusion, infiltrative changes, baseline shift, tumor progression and tumor regression can occur for patients with lung cancer and are each given a code for registration. For each of these changes, there are separate associated guidelines for what color the patient should be handed. The study by Kwint et al. described earlier [46] evaluated their protocol on 1793 CBCT-scans of the 177 lung cancer patients. The 72% with ITACs were categorized as red, orange or yellow.

3 Materials and methods

This thesis was based on evaluation of HUHs traffic light protocol for LA-NSCLC. The patient data used was from the pulmDIBH-study at HUH, a study approved by the Regional Committee for Medical and Health Research Ethics of Western Norway (REK 2019/749). By recalculation of the patient's treatment plan on CT scans taken during treatment, we evaluated how well the treatment plan worked over the treatment course and if the clinical traffic light registrations matched. In this chapter, the patient material and procedure of the recalculation are presented. Methods for evaluation of the recalculated treatment plans are included, as well as methods for statistical evaluation of the traffic light protocol.

3.1 Materials used in this thesis.

3.1.1 Patients

Patients at HUH with inoperable stage III NSCLC, treated with photon IMRT in the period of October 2019 until May 2022, were invited to participate. The patients involved in the study signed informed consents forms. In total, 45 were included in the study after some of the patients had to be excluded of different reasons. In this thesis 41 patients were available for research, since two of the patients did not have all structures delineated yet, one patient with stage 4 (IV) had spread to the heart and is thus not representative, and one patient was not fit to have CT scans in week 1 and 3. For this current project, the patient data were de-identified before they were available for the candidate. Patient characteristics are represented in table 3.1.

Table 3.1: Characteristics of the patients included in this thesis. The majority of patients had IIIA or IIIB LA-NSCLC and most patients received concurrent chemotherapy.

Stage	Number of patients
IB	1
IIA	1
IIB	2
IIIA	15
IIIB	17
IIIC	3
IVA	2
Target Volume	
Tumor + nodes	31
Primary tumor only	9
Nodes only	1
Primary tumor location (lobe)	
Left upper	**7**
Left lower	10
Right upper	15
Right upper + middle	1
Right lower	8
Prescribed dose	
60 Gy	14
66 Gy	26
70 Gy	1
Chemotherapy	
Sequential	2
Concurrent	39
Sex	
Female	18
Male	24
Age average	**Age range**
67	53-82

3.1.2 CT imaging

As a part of clinical practice, planning CT (pCT) scans were taken to make treatment plans for each patient. For the purpose of the pulmDIBH-study, additional CT scans were acquired at planning and also during treatment. Standard treatment was delivered during free breathing and the pCT scans were therefore AIP of ten breathing phases of 4DCT scans. However, the patients were also imaged with DIBH CT scans as a part of the pulmDIBH, and DIBH treatment was available if the responsible oncologist anticipated DIBH to be better. Both DIBH and AIP are described earlier in the theory part of this thesis (chapter 2.4.1 and 2.4.2).

Repeat CT scans (rCTs) were taken the first and third week of the treatment. The rCTs were taken in close connection to the treatment fraction the same day. The rCT scans included both a 4DCT and DIBH CT, and the timeline of collection of CT scans is illustrated in figure 3.1.

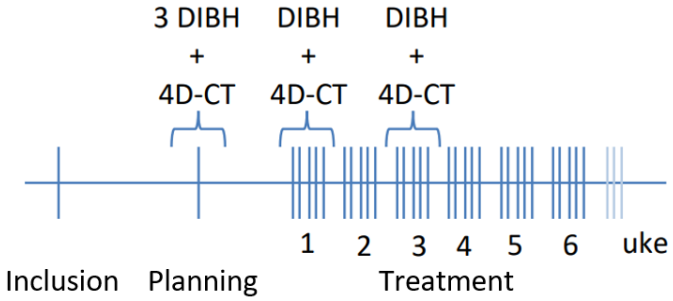

Figure 3.1: Timeline of CT scans for the study. Five fractions each week are represented as vertical lines. For each treatment fraction a CBCT scan was taken to evaluate if the patient were in need of adaptation by the traffic light protocol, and to adjust patient setup. DIBH and 4D-CT scans were taken in the planning phase, but also as rCTs week 1 and week 3.

Three of the patients did not take the rCT in week 3. One because of an infection, one because of COVID-19 restrictions, and the last patient ended the treatment course after 13 fractions.

3.1.3 Delineation and planning

The responsible oncologist delineated structures on the AIP pCT, while the dedicated oncologist delineated the DIBH pCT and the rCTs (both AIP and DIBH) in week 1 and week 3. The responsible and dedicated oncologists could be the same person for some of the patients. This was done on both the AIP and DIBH scans regardless of which strategy the patient received treatment by. CTV, PTV, IGTV and GTV were important structures delineated by the oncologists. Delineation of OARs like spinal cord, lungs, heart, and esophagus was performed by the responsible dosimetrist, and controlled by the responsible oncologist. Brachial plexus is also an OAR for patients with target volume located in the upper part of the lungs.

The prescribed dose was between 60 and 70 Gy, usually 60 or 66 Gy, depending on the patient's tumor location and overall health. OARs relative to the tumor were considered when prescribing the dose. A total dose of 60 Gy was often prescribed to patients with target volume near brachial plexus, or if it was hard to maintain other dose limits for OARs. The prescribed dose was planned for 30-35 fractions, delivered with standard fractionation of 2 Gy.

IMRT plans for clinical use were made in the treatment planning system Eclipse (Varian Medical Systems, INC. Palo Alto, CA USA) by a dosimetrist. Photon radiation of 6 fields and energy of 6 MV were normally used. Two of the patients involved in this study received VMAT treatment because the IMRT plan was not sufficient.

Ten patient treatments were planned on the DIBH CT, while the rest were planned on the AIP of the 4DCT. DIBH planning and treatment were given to patients with irregular respiratory motion and cases with risk of too high lung dose. One of the patients had two separate IMRT plans, because of the distance between the primary tumor and one of the metastases in the mediastinum. The distance made it difficult for the MLC to shield the area between them, so one IMRT plan would risk high doses of radiation to normal tissue and OARs. A plan for the primary tumor and another for the metastasis were thereby made.

3.1.4 Traffic light protocol

HUH uses a traffic light protocol for ART of patients with lung cancer, and the protocol is similar to the one developed by Kwint et al. [46]. The protocol was implemented when the pulmDIBH study was started, and a RTT assigned a traffic light color to each patient based on the anatomical evaluations of the CBCT scan acquired in advance of each treatment fraction. The protocol had intentions of deciding if the patient needed adaptations in the form of a new treatment plan (replan). The protocol is represented in Appendix B. Green color registration represented small or no anatomical change, and yellow represents some change that was noted. Orange color registration triggered *control CBCT-task*, where a physicist needed to consider the need of a replan together with an oncologist. Red color stopped the treatment until a physicist and an oncologist had evaluated the situation. The protocol was implemented for every fraction of the whole treatment course, and over 1000 traffic light registrations were made in total for the 45 patients in the pulmDIBH study.

The traffic light registrations were based on bone-matching, where the CBCT was compared to the pCT based on anatomy of the patient's bones. Usually, the patients were also treated in a position setup based on bone-match. Anatomical changes, like baseline shift larger than 5 mm, could lead to a bad treatment outcome, but it was not always necessary with a replan. The patient could then be treated in a different position setup, based on soft-tissue instead of bones. CTV match, or an intermediate setup between CTV and bone-match, could be an alternative for these patients. CTV-match and intermediate match got *tumor-match* as collective term for

this thesis. The treatment table was then moved in three directions to adjust to the new match. This resulted in a shift of isocenter, hopefully closer to the center of the CTV, leading to better CTV coverage. The shift (lateral, vertical, and longitudinal direction) was noted for the patient.

The candidate was only studying the traffic light registrations of the days of rCTs (week 1 and week 3) for the 41 patients included. This was because dose recalculation on CBCTs came with uncertainties and were less accurate than for conventional CT. The rCTs were only taken in week 1 and week 3 for the purpose of the pulmDIBH study. This means that all data are cross-sectional data. The rest of the traffic light protocol registrations are not included and may vary between our two cross-sectional data. The same goes for the dosimetric parameters withdrawn from the recalculations of the rCTs.

3.2 Methods applied in this thesis.

3.2.1 Image registration

To recalculate a treatment plan on another CT scan than the pCT, the two scans needed to be spatially aligned. To spatially align the two scans, the coordinate systems of the two sets of images were matched. This was done in the Image Registration system in Eclipse, and the process is hereby referred to as image registration. In this study, image registration of the rCT from week 1 and week 3 was made by the candidate. To make an "auto match" between two scans, a "source image" and a "target image" had to be selected, where the target image was the scan that was aligned to the source image. Here, the source was the pCT and target was the chosen rCT. The pCT and rCT were either AIP or DIBH scans, depending on what the clinical treatment was based on for each patient.

Some patients got a re-plan during the treatment course. For example; the re-plan could be received clinically between week 1 and 3, and was planned based on a new CT scan or the week 1 scan (as the newest scan). Week 1 image registration would be matched with the original pCT, but week 3 image registration should then be matched with the newest CT scan (as pCT for the re-plan).

The image registration can be made with focus on bone anatomy or soft tissue. For the patients in this study the candidate made image registrations matched by bone anatomy, since it was the type of match the traffic light protocol CBCT was based on. Treatment delivery was also usually given by bone-match, but tumor-match (soft tissue) could be an alternative as mentioned earlier.

When bone structure was selected, the program performed the auto match with intensity range between 200 and 1700 HU. The two images were then moved in three dimensions (vertical, longitudinal, and lateral axes) to align the scans based on the HU range. The match could be improved by editing the volume of interest (VOI), i.e where the program should focus. The VOI is shown as the red box in figure 3.2, where CTV for both scans is shown in pink. For each image registration the box was edited in all three dimensions to frame the CTV and bone structure nearby like the spine and some of the ribs. The volume of the box was naturally edited differently for each registration, depending on CTV size and location.

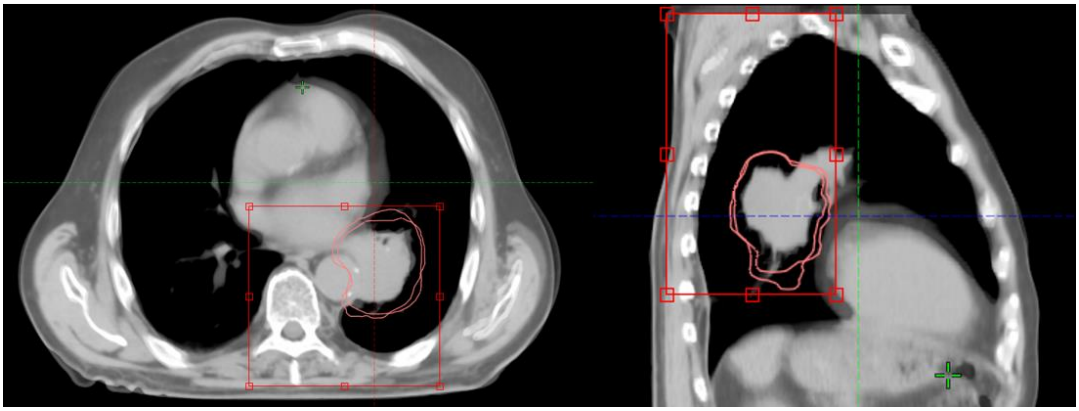

Figure 3.2: VOI for image registration in Eclipse, represented as the red box. CTV delineated for pCT and rCT, both delineated in pink. Prioritizing the CTV together with the spine + some of the ribs as VOI, to get the most sufficient match for this patient.

From here, the match was studied closely, slice by slice through the body. If the transitions between the scans were abrupt when studying bone structures, it was not a good match in that exact area. This could be that a bone structure from the rCT was located on top of soft tissue from the pCT. Ideally, each bone of the CT scans would align perfectly, but this was rarely the case because of reasons like motion or if the patient's body shape had changed over the week(s) between the CT scans. The spine and ribs near the CTV were prioritized when the quality of the match was evaluated.

Each image registration, usually two per patient (week 1 and week 3), was saved after evaluation. Some of the image registrations were evaluated together with the candidate's supervisor. These registrations were harder to get sufficient, because of different reasons. Some patients had a slightly curved position on one of the images, and some patients had different breathing levels on the two images. The match was either sufficient for the ribs or the spine area for these patients, and it was not possible to prioritize both in the VOI. Prioritizing the spine area was discussed with the candidate's supervisor and implemented as a solution for these patients.

The candidate did 42 image registrations in total for 22 of the 41 patients included in this thesis. The other 19 patients had image registrations and recalculated dose distributions made by an earlier master student, carried out with the same procedures [54].

3.2.2 Recalculation of the treatment plan in External Beam Planning

Recalculation of treatment plans was done in the External Beam Planning system in Eclipse. The clinical treatment plan was then copied and transferred using the image registrations for the rCTs. Using the same treatment fields and monitor units, the dose distribution was recalculated. Due to possible changes in tissue densities for the rCTs, the dose distribution would then be different than for the pCT. Anatomical changes could occur differently during the treatment course, and the dose distribution could thereby differ week 1 and week 3.

If there was a re-plan during the first three weeks of the treatment course, the fields and monitor units of the re-plan were copied to the rCT instead of the original plan. Recalculation with the re-plan was implemented if the re-plan was received clinically at the time of the rCT.

Three treatment plans were now available; the plan calculated on the pCT, week 1 scan, and week 3 scan. Re-plan distribution week 3, for the replan patients. Figure 3.3 represents dose distribution of pCT, week 1 and week 3 scans in External Beam Planning for patient 15.

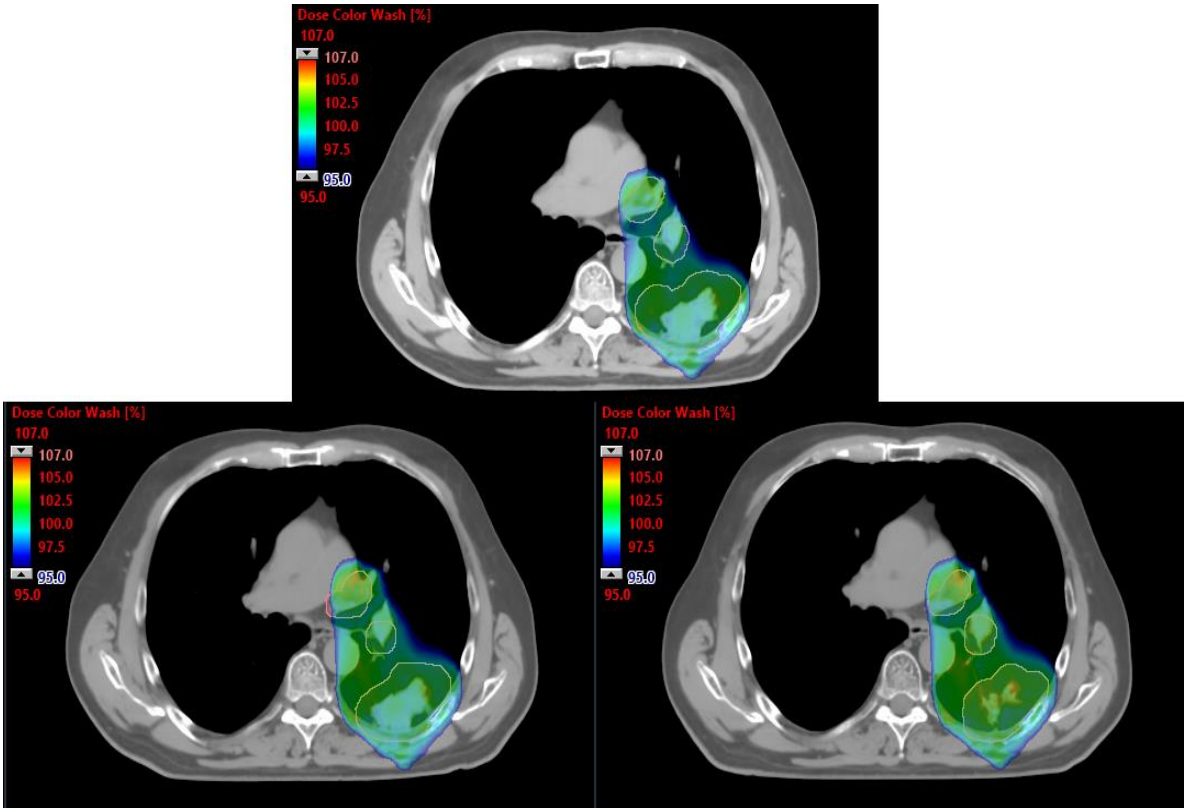

Figure 3.3: Dose distributions for planning (top), week 1 recalculation (bottom left), and week 3 recalculation (bottom right). Pasient nr 15 here, showed a different dose distribution in the same cross section of the body. Delineation of CTV structure also changed during (pink delineation).

Recalculation week 3 was naturally not possible for the three patients who did not have rCT week 3.

3.2.3 Plan evaluation

To evaluate the treatment plan, dose distributions and DVHs for some defined volumes like CTV, PTV, the whole body, spinal canal, heart, lungs, and esophagus were studied. Brachial plexus were not studied since most patients did not have tumors nearby. The parameters collected from the DVHs and used in this thesis are shown in table 3.2, with associated clinical goals.

Table 3.2: Parameters/clinical goal collected for each patient. The parameters/clinical goals are a mix of parameters used clinically at HUH, and inspired by Hoffmann et al. study [55] and Møller et al. study [56].

Structure	**Parameter/goal**
CTV	V 95% ≥ 99 %
CTV	D 98 % ≥ 95%
PTV	V 95% ≥ 98 %
PTV	D 98 % ≥ 95%
BODY	D 0.1 cm^3 ≤ 107 %
BODY	V 107 % ≤ 0.1cm^3
Spinal Canal	D 0.1 cm^3 ≤ 50 Gy
Heart	D_{mean} ≤ 35 Gy
Heart	D 0.1 cm^3 ≤ 66 Gy
Lungs	D 0.1 cm^3 ≤ 107 %
Lungs	D_{mean} ≤ 20 Gy
Esophagus	D 0.1 cm^3 ≤ 66 Gy
Esophagus	D_{mean} ≤ 34 Gy

V95% is the volume that receives 95% of the prescribed dose, and for CTV this volume should be at least 99% of the total volume. Table 3.2 also shows a parameter goal: V 107 % ≤ 0.1cm^3 for the whole body. This parameter represents how much volume that receives 107% of the prescribed dose and it is preferable that this volume is less or equal to 0.1 cm^3. In some cases, tissue outside PTV will receive a relatively large dose, and a volume that gets a dose larger than 100% of the specified PTV dose is referred to as a Hot Spot [34].

D_{mean} ≤ 35 Gy for the heart means that the mean dose of the heart should be equal or less than 35 Gy. D 0.1 cm^3 ≤ 50 Gy for the spinal canal, describes how it is preferable that a volume of 0.1 cm^3 receives less than 50 Gy. These limits vary among the OARs, depending on how sensitive the tissue is to radiation. All the parameters in table 3.2 were collected for each plan for each patient (planning, week 1, and week 3). To collect these parameters, the clinical goal function in Eclipse was used. The dosimetric changes during the treatment course were studied by these parameters. The clinical goal parameters and traffic light registrations, respectively, were merged together for the patient with two treatment plans. This was decided to not complicate the analysis. For all the 41 patients, 120 sets of clinical goals with 120 associated traffic light registrations, were collected for comparison and evaluation of the protocol.

Sources of clinical goal failure

If some of the recalculations did not pass the clinical goals represented in table 3.2, these patients were studied even more closely to evaluate some possible reasons for this. First of all, the CTV parameters of V95 and D98 were studied, and there could be different reasons why the dose was lower than desired. The clinical goals could be failing for one or both weeks, and the plan(s) that failed were then studied in External Beam Planning in Eclipse. Looking at the different delineated volumes, like CTV especially, and how it may have changed position and/or size.

The candidate compared the scans (pCT and rCTs), how the patient's anatomy changed while also reading comments from the traffic light protocol. If the traffic light protocol registrations showed anatomical changes compared to the pCT, it could be a natural cause behind the clinical goal failure. Since it was not recalculated a dose distribution before each fraction clinically, the dosimetric consequences were not always clear by just studying the CBCT. Different other sources for the clinical goal failure are represented below and were discussed with the candidate's supervisor. Together with the candidate's supervisor, it was evaluated that some of the patients needed to be withdrawn from the study of traffic light correlations.

Image registration

As mentioned, some image registrations were harder to do sufficiently with a bone-match. The patients with big position differences between the two scans were registered with a decent bone-match of the spine, but not as good a match for the ribs. For example, the patient's back could be more curved in week 1 rCT than for the pCT, and then the dose distributions would have its differences when recalculating.

Breathing level

The radiation treatment came with a risk of receiving dose delivery in another breathing level than as planned. The pCT and rCT could be taken in different DIBH levels, e.g the patient filled their lungs more in one of the scans. This was also a risk with free-breathing treatment. A baseline shift could be a result of this. By using a box located on top of the sternum as an external marker, the DIBH patients could hold their breath within a 3 mm window level. The anatomical positions within the thorax could still vary some.

Delineation

The supervisor made the candidate aware of a possible error originating from delineation. Oncologists follow guidelines and directions of delineation, and these directions can develop over time. There is a suspicion that some patients could have pCT delineation practiced by other guidelines than the ones usually used in the clinic.

Learning curve in implementation of the traffic light protocol

With implementation of the traffic light protocol, there comes a learning curve for the RTTs that could impact the traffic light registrations of the first patients included in pulmDIBH. In order to correct for this uncertainty, an experienced RTT re-did the traffic light registrations of the initial 19 patients off-line. New traffic light registrations were then made for week 1 and week 3. The treatment could have been affected if these registrations were made during the treatment course, for example by triggering a replan. When the RTTs evaluated CBCTs clinically for the other patients, the ones after the first 19, they were probably more experienced. That is why re-evaluation was only carried out for the first 19 patients.

Tumor-match

Some of the patients were given treatment based on a tumor-match instead of the bone-match. The dose distribution and clinical goal parameters collected were based on bone-match treatment, and switching to tumor-match treatment could influence the clinical goals. This will be evaluated later in this thesis, when recalculation of the treatment plan was executed by tumor-match instead of bone-match.

Overlap between CTV and OARs

Some patients might have OAR doses just above the clinical goals. The tumor might then be close by and sometimes the CTV overlaps with the OAR. Typically, this could be OARs as the heart and/or esophagus. Irradiating CTV with enough dose is prioritized, even though it risks increasing the dose to OARs, as long as the risk of normal tissue toxicity is under control. How this relationship is handled depends on how wide the therapeutic window is and the goal of the treatment. All the patients included in this study were treated with curative intent, which means that sparing normal tissue (especially OARs) was important, but at the same time the CTV needed a high enough dose for the curative intention.

Hot spots

Hot spots are explained earlier in this chapter and could be a possible reason for clinical goal failure. If the hot spot is located at the same area for each fraction, the total dose to this specific area would be very high and a possible danger for the patient, especially if it is located in OARs or other normal tissue. Hot spots are not that dangerous if they are located differently for each fraction, since the high doses are distributed over a bigger area. This avoids a large total dose for a small volume and decreases the risk of normal tissue complication. Perforation of esophagus could be a consequence and could be severe and life threatening.

3.2.4 Statistical evaluation

IBM SPSS Statistics 26 was used for the statistical evaluation of the results. The program was used to evaluate differences between the original treatment plan and the recalculated plans in week 1 and week 3, and to study correlations between the traffic light protocol registrations and parameters found. The Friedman's Two-Way Analysis of Variance (ANOVA) by Ranks was practiced for analysis of planning, week 1 and week 3 parameter differences. This is a nonparametric test used to determine statistically significant differences when comparing multiple groups [57]. It was evaluated if there was a significant change between the three groups (planning, week 1 and week 3), with a significance level of $p = 0.05$. The groups were also put through a pairwise comparison with p-values adjusted by Bonferroni correction. The Bonferroni correction is supposed to adjust for the problem of type I error then the number of tests increases [58]. Type I error is that the test concludes significant differences in the data, when there are not. IBM SPSS Statistics 26 was also used to make correlation graphs between datasets.

3.2.5 Evaluation of tumor-match patients

15 patients received treatment based on tumor-match week 1 and/or week 3. To evaluate if this gave a better treatment, the already recalculated treatment plan (with bone-match alignment) was adjusted for the isocenter shift in External Beam Planning. The dose distribution was recalculated again and evaluated together with how the new isocenter had moved with respect to the CTV. The clinical goal parameters in table 3.2 were also collected for these new tumor-match based recalculations, and then compared to the result for the bone-match recalculations. This procedure was performed on 21 recalculations for the 15 patients who received tumor-match clinically week 1 and/or week 3.

This recalculated dose for tumor-match represents better what these patients received clinically, than the bone-match recalculation did. So lastly, estimated delivered dose during treatment was evaluated (exchanging in the dosimetric values associated with the tumor-match recalculation for these patients). This mix of bone-match recalculations and tumor-match recalculations made a clinical approximation. The clinical availability of tumor-match treatment was evaluated, to see if it had a purpose for this group of patients.

4 Results

4.1 Traffic light protocol results

Figure 4.1 represents the frequency of the different traffic light colors for week 1, week 3, and in total for them both. It was an increase of the color yellow from week 1 until week 3, but a decrease of the color orange. For those two colors together, the number increased from week 1 ($N = 22$) until week 3 ($N = 28$).

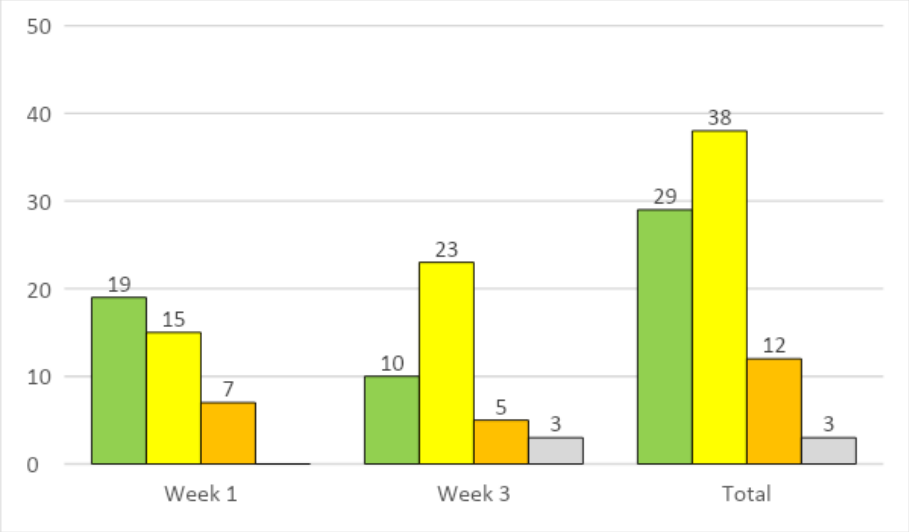

Figure 4.1: Frequency of traffic light color registrations week 1, week 3, and in total. Green, yellow, and orange represented. No red color registered clinically. Three of the patients did not take the rCT in week 3 (represented here as the color gray: no traffic light registration).

In general, there were more reports of anatomical changes in week 3 ($N = 29$) than in week 1 ($N = 26$). Distributions of anatomical changes present week 1, week 3, and in total are represented in table 4.1. There were in total 29 traffic light registrations that did not receive any code of anatomical change, where five of them were registered as yellow and one of them as orange.

Table 4.1: Codes of anatomical changes reported from the traffic light protocol for all patients week 1, week 3, and in total. Cases of no anatomical changes reported were 29, and are not represented in the table.

Traffic light code	Week 1	Week 3	Total (%)
Atelectasis	0	1	1 (1.8)
Pleural effusion	0	0	0 (0)
Infiltrative changes	0	0	0 (0)
Baseline shift	23	19	42 (76.4)
Tumor progression	1	1	2 (3.6)
Tumor regression	2	8	10 (18.1)
Total	26	29	55 (100)

As a result from the traffic light protocol, five patients (12.2%) received a replan between week 1 and week 3 rCT. These patients had baseline shift, tumor regression or tumor progression present in-between the rCTs, and decision of a replan was made based on the protocol.

Fifteen patients received treatment based on CTV match ($N = 12$) or an intermediate match ($N = 3$) week 1 and/or week 3. 21 treatments in total (8 orange, 12 yellow, and one green) were reported in need of tumor-match treatment. 16 of them had baseline shift observed (tumor regression also present for one of them), and the other five did not receive a traffic light code.

Baseline shift was observed in 30 patients (73.2 %), where week 1 ($N = 23$) had a few more cases than week 3 ($N = 19$). Most were registered as yellow ($N = 27$), some orange ($N = 10$), and a few were green ($N = 5$). Four of the reports of baseline shift also included tumor regression, and one patient with baseline shift also had **atelectasis**. This was the only patient reported with atelectasis.

Tumor regression was observed in 8 patients (19.51%), and most cases in week 3 ($N = 8$) compared to week 1 ($N = 2$). All cases in week 1 were level green, and all cases in week 3 were level yellow. Only two patients (4%) were observed with **tumor progression**, one week 1 were level yellow and one week 3 were level orange.

4.1.2 Updated registrations after off-line review

This part is a representation of how traffic light registrations could look like if HUH implemented a test system, or more training of RTTs before evaluating the first 19 patients. The re-evaluated registrations are present here. Of all the re-evaluated traffic light protocol registrations ($N = 37$), 24 were labeled the same color, 8 changed from green to yellow, 1 green to orange, 1 green to red, 1 yellow to orange, 2 orange to yellow. Only two were downgraded in color level, and the rest got a higher level.

19 registrations were re-evaluated with the result of the exact same presence of anatomical change (registered code). 8 registrations with no code present were re-evaluated to get one, mostly baseline shift, but also one tumor regression and one tumor progression. Only 16 (43.2%) registrations kept both their exact color and code after the evaluation.

All the traffic light registrations for these first 19 patients are now replaced with new ones, and the registrations for the last 22 patients are still the same. Figure 4.2 shows the updated color registrations and table 4.2 represents the updated code registrations, of week 1, week 3, and in total.

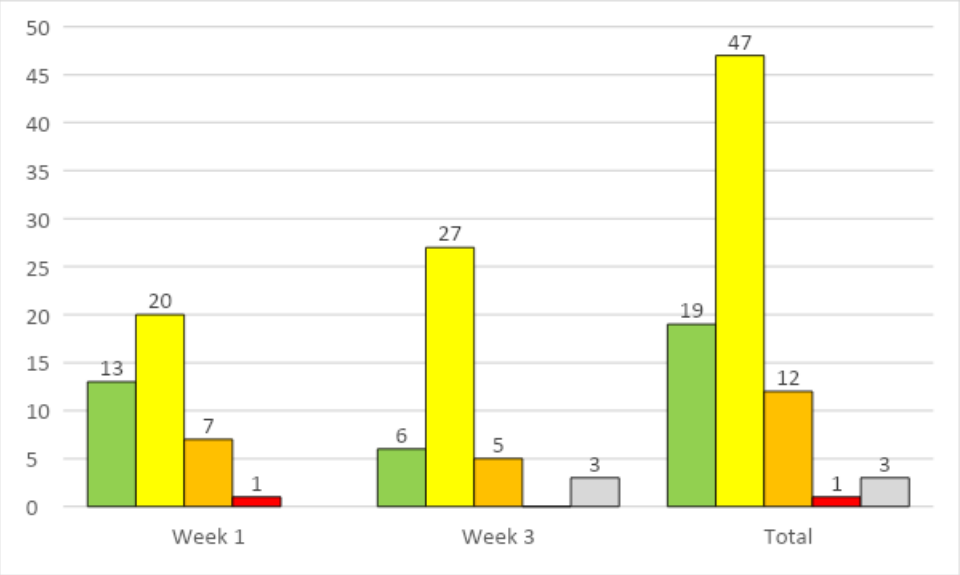

Figure 4.2: Frequency of traffic light color registrations (after re-evaluation) week 1, week 3, and in total. Green, yellow, and orange represented as earlier. Now red traffic light registrations are present. Grey are still representing the patients who did not take the rCT week 3.

Compared to the registrations made clinically, there was an increase of level yellow ($\Delta N = 9$) and decrease of level green ($\Delta N = -10$). The amount of orange registrations were the same, but there was now one red registration compared to zero earlier. The patients that did not get an rCT in week 3 are still represented in the graph with gray color, even though they did not get a traffic light registration (and then naturally did not get a re-evaluation). One of these three patients got a re-evaluation of week 1.

Table 4.2: Updated registrations (after re-evaluation) of anatomical changes (codes) present week 1, week 3, and in total.

Traffic light code	Week 1	Week 3	Total (%)
Atelectasis	2	3	5 (7)
Pleural effusion	0	0	0 (0)
Infiltrative changes	0	0	0 (0)
Baseline shift	24	21	45 (67)
Tumor progression	2	1	3 (5)
Tumor regression	3	11	14 (21)
Total	31	36	67 (100)

In general, more anatomical changes were observed and reported ($\Delta N = 12$) after re-evaluation. There were still zero cases of pleural effusion and infiltrative changes, and there was an increased report of every other code (atelectasis; $\Delta N = 4$, baseline shift; $\Delta N = 3$, tumor progression; $\Delta N = 1$, tumor regression; $\Delta N = 4$).

4.2 Estimated dose assuming bone alignment

Mean, median and interquartile range (IQR) values for V95 and D98 for CTV for planning, week 1 and week 3 are represented in table 4.3.

Table 4.3: Mean, median, and IQR values for CTV V95 and CTV D98 for all patients. Values represented for planning, week 1, and week 3.

Parameter	Planning	Week 1	Week 3
Mean V95 [%]	100	98.7	98.9
Median V95 [%]	100	99.7	99.8
Q3 – Q1 (IQR) V95	$100 - 100$ (0)	$100 - 98.9$ (1)	$100 - 99.4$ (0.6)
Mean D98 [%]	98.8	93	93.5
Median D98 [%]	98.8	98.0	98.2
Q3 – Q1 (IQR) D98	$98.9 - 98.7$ (0.2)	$98.7 - 96.2$ (2.5)	$99 - 97$ (2)

With a significance level of 0.05, the Friedman's ANOVA test showed a significant change in CTV V95 between planning, week 1, and week 3 ($p = 0.000$), and the null hypothesis (that the distributions of CTV V95 are the same) were rejected. Pairwise comparison with Bonferroni correction did not result in a significant difference between week 1 and week 3 ($p = 0.561$). Between planning and week 1 ($p = 0.000$), and planning and week 3 ($p = 0.000$), there was a significant difference, i.e CTV coverage was significantly better for planning, than week 1 and week 3.

The mean value of CTV V95 for the five patients receiving replan increased from 96.9% week 1 to 99.5 % week 3.

CTV D98, had also significant change between planning, week 1 and week 3 ($p = 0.000$). Pairwise comparison with Bonferroni correction resulted in significant change between planning – week 1 ($p = 0.000$) and planning – week 3 ($p = 0.010$), but not for week 1–week 3 ($p = 0.364$). Figure 4.3 and 4.4 shows box plots of CTV V95 and CTV D98, respectively, in the planning, week 1 and week 3 for all patients. Patients 31, 34, and 39 were the three of the most extreme outliers for both parameters, both weeks.

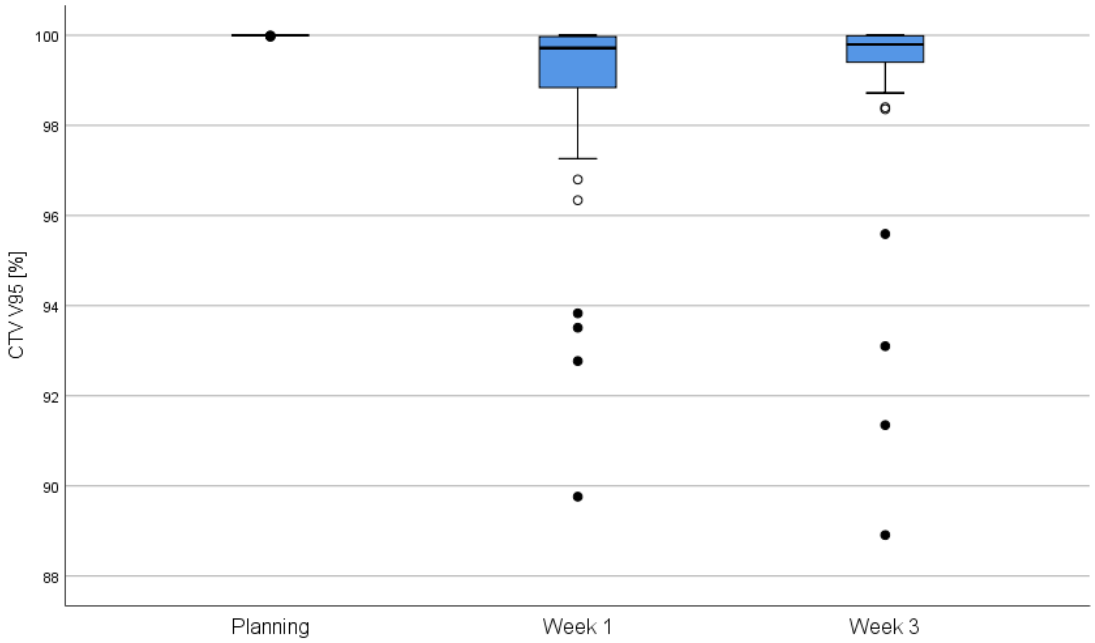

Figure 4.3: Boxplot of CTV V95 [%] for planning, week 1, and week 3. The box plot illustrates the interquartile range, and the bold black line represents the median. Filled dots equal's extreme outliers, while hollow represents mild outliers.

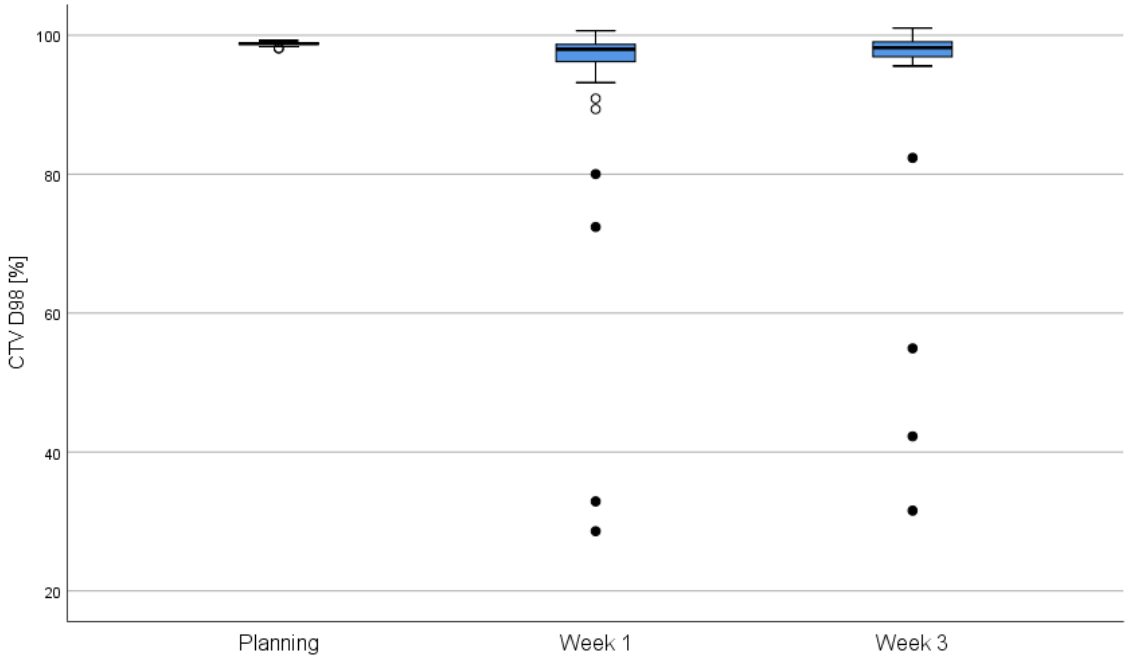

Figure 4.4: Boxplot of CTV D98 [%] for planning, week 1, and week 3. The box plot illustrates the interquartile range, and the bold black line represents the median. Filled dots equal's extreme outliers, while hollow represents mild outliers.

For V107 for the body, there was a significant difference between planning and week 3 ($p = 0.007$) after adjustment by the Bonferroni correction, but not between planning and week 1 ($p = 0.101$). Between week 1 and week 3 there was no evidence for rejecting the null hypothesis ($p = 1.00$), which means there was no significant difference. Figure 4.5 shows a boxplot of V107 body for planning, week 1, and week 3. As the boxplot shows there are multiple outliners for both week 1 and week 3, which contributes to the p-value equal to 1 between them. All of the patients who are outliers of week 3, are also outliners week 1. The most extreme outlier of week 3 is patient 30.

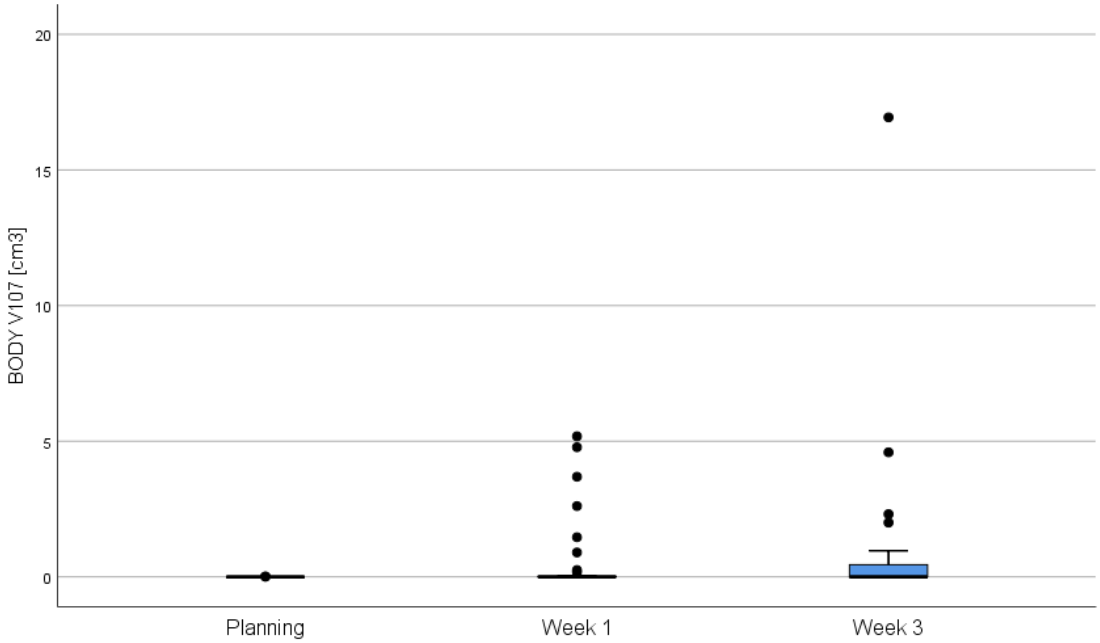

Figure 4.5: Boxplot of BODY V107 [cm^3] for planning, week 1, and week 3. The box plot illustrates the interquartile range, and the bold black line represents the median, which is close to zero for all. Filled dots equal's extreme outliers.

Table 4.4 shows mean values of Body and OAR parameters for all patients in planning, week 1 and week 3.

Table 4.4: Mean values for Body and OAR parameters. Calculated from all patients' clinical goal parameters in planning, week 1 and week 3.

Parameter	Planning	Week 1	Week 3
Body V107 [cm^3]	0	0.47	0.82
Body D0.1cm^3 [%]	103.88	105.80	106.52
Esophagus D0.1cm^3 [Gy]	62.27	62.12	63.02
Esophagus D_{mean} [Gy]	20.41	20.01	21.38
Heart D_{mean} [Gy]	9.66	9.80	9.69
Heart D0.1cm^3 [Gy]	61.88	61.77	62.32
Lungs D0.1cm^3 [%]	102.84	104.69	105.09
Lungs D_{mean} [Gy]	14.05	14.14	14.17
Spinal Canal D0.1 cm	40.21	40.34	40.62

Table 4.5 shows how many patients that failed different clinical goals from table 3.2, for week 1 and week 3 recalculations.

Table 4.5: Number of clinical goal failure for all patients. Most of the clinical goals from table 3.2 are present. Clinical goals of PTV were not studied further, CTV was decided as representative enough for target coverage. Have in mind that three of the patients from week 1 are not present week 3.

Clinical goal	Week 1	Week 3	Total
CTV V95% ≥ 99 %	12	7	19
CTV D98 % ≥ 95%	8	4	12
BODY D0.1 cm^3 ≤ 107 %	8	14	22
BODY V107 % ≤ 0.1cm^3	8	14	22
Spinal Canal D0.1 cm^3 ≤ 50 Gy	2	0	2
Heart D_{mean} ≤ 35 Gy	0	0	0
Heart D0.1 cm^3 ≤ 66 Gy	17	15	32
Lungs D0.1 cm^3 ≤ 107 %	7	6	13
Lungs D_{mean} ≤ 20 Gy	1	0	1
Esophagus D0.1 cm^3 ≤ 66 Gy	15	13	28
Esophagus D_{mean} ≤ 34 Gy	2	1	3

Twelve (29 %) patients failed one or both CTV goals week 1, and 7 (17%) patients failed one or both goals week 3. Four out of the twelve who failed a CTV goal week 1, got a replan. This means that one of the patients that received a replan, had sufficient target coverage week 1, in advance of implementation of the replan. This is patient 13, who also did not fail any other goal represented in table 4.5, but received a replan because of technical problems.

4.2.1 Patient cases

Table 4.6 below, represents some of the patients with especially low values for one or multiple of the V95 and/or D98 parameters for CTV during week 1 or week 3. The numbers marked in red are parameters below the associated clinical goal. Traffic light registration for week 1 and week 3 for each patient is also included.

Table 4.6: Some patient cases with low target coverage for week 1 and/or week 3. Target coverage is represented by D98 and V95 for CTV. Traffic light registrations given clinically are also present in the table. Numbers marked by red color are below constraints of the clinical goal.

Patient number	CTV D98[%] Week 1	CTV V95[%] Week 1	Traffic light	CTV D98[%] Week 3	CTV V95[%] Week 3	Traffic light
16	80,02	92,8		96,48	98,7	TV
20	89,37	96,3		95,75	98,4	B
23	93,17	97,26	TV	97,73	99,87	
25	94,8	97,89	B	99,5	99,72	
31	28,6	89,8	B	42,26	91,35	B
34	32,89	93,8		31,56	93,1	
39	72,4	93,51		54,93	88,91	B

Traffic light protocol error - patient 16

This patient had a large tumor, and the volume of CTV increased from 1316.78 cm^3 (pCT) to 1578,88 cm^3 (week 1) and 1554,47 cm^3 (week 3). Figure 4.6 represents the tumor progression between the pCT and rCT in week 1 by one slice of the CT scans in a frontal view. The top image is the pCT with CTV delineated in pink. The bottom image is the rCT week 1, with the plan CTV still at the same position, and week 1 CTV delineated in a thinner pink line.

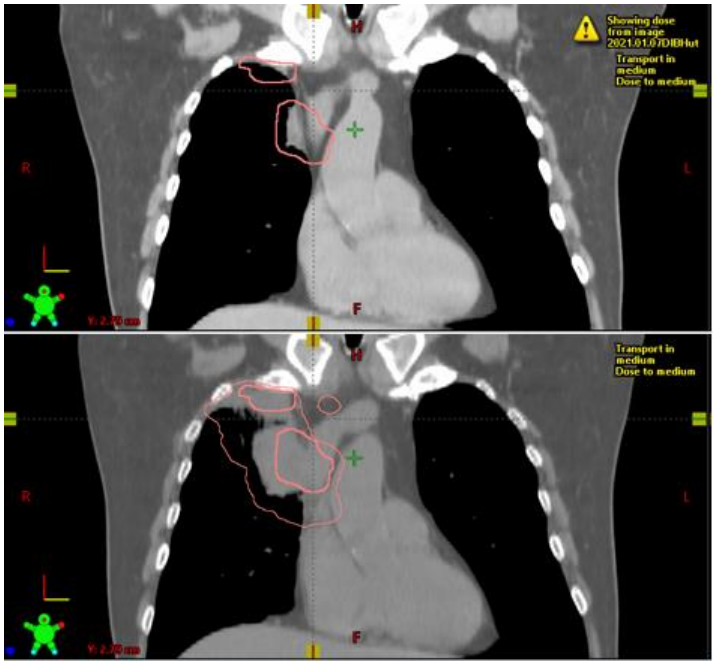

Figure 4.6: Tumor progression of patient 16 between pCT and rCT week 1, with a frontal view. CTV increased from 1316.78 cm^3 to 1578.88 cm^3 from week 1 until week 3.

The tumor progression was not detected until import of week 1 rCT, and the patient then got a replan based on this rCT. This patient was one of the 19 patients who got a new traffic light evaluation after the treatment ended. The new evaluation of week 1 rCT resulted in a code red with tumor progression and baseline shift. For this patient, there was a major error from the protocol when a green registration should have been a red one.

Tumor-match - Patient 20

This patient received treatment based on tumor-match in week 1 and week 3. The traffic light protocol categorized both rCTs as orange. The CTV coverage was improved in week 3 compared to week 1, but the baseline shift code did not take place until week 3.

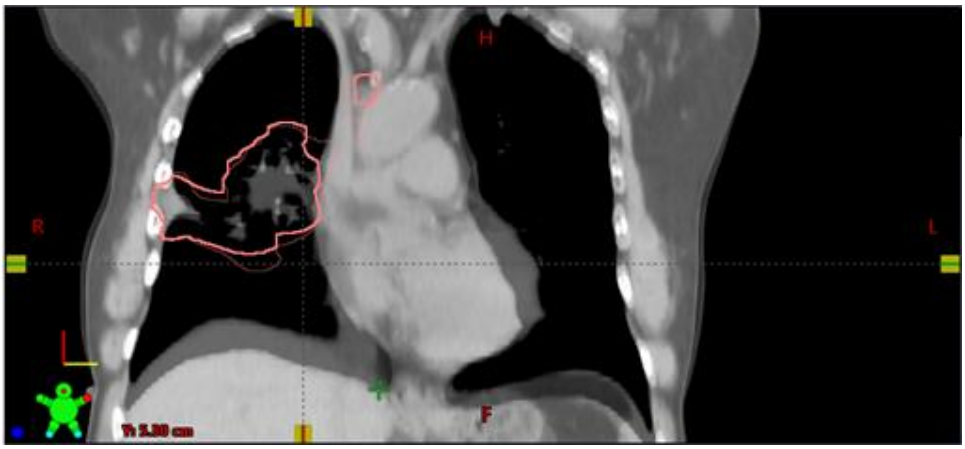

Figure 4.7: Planning (thick pink line) and week 1 (thin pink line) delineation of CTV for patient 20, in a frontal view.

Figure 4.7 shows a frontal view slice of patient 20 from week 1 rCT, with CTVs delineated in pink where week 1 CTV has a thinner line than for the planning CTV. It can also be mentioned that this is an example of a possible DIBH error as well, the shadow from the pCT has a different DIBH level than for the rCT in week 1.

Delineation error - Patient 31 and 34

Patient number 31 and 34 were the two patients who got delineations that did not follow the study protocol. Figure 4.8 shows the pCT for patient 31, represented with both oncologist's CTV delineations. The thin pink line is the CTV delineated according to protocol, and the thicker pink line is the delineated according to (possible) old guidelines. As the figure shows, the different guidelines resulted in quite different delineations for this patient.

Figure 4.8: Delineation of CTV on the pCT of patient 31 in a frontal view. CTV delineated according to protocol represented by the thin pink line, and the thicker pink line is the CTV delineated according to (possible) old guidelines. The thick line was the delineation used clinically when evaluating CBCTs.

The treatment plans for these two patients are based on delineations following the (possible) old guidelines. The structures of rCT, delineated according to updated guidelines, has a dose that is affected from this planning error. The CTV week 1 and week 3, received a dose that was too low. It still represented a dose the patient received clinically, so the parameters could be used in the general analysis of the treatment plans.

The traffic light registrations were, on the other hand, based on the pCT delineation (from old guidelines). So, the RTT who compared the CBCT to the pCT, gave the registration based on delineations not supported by study protocol. This registration cannot be compared to the parameters that represent delineation supported by study protocol. These two patients were thereby excluded in the statistical evaluation of the traffic light protocol.

Overlap and hot spots - patient 28

Patient 28 was a classic example of how tumors of LA-NSCLC could be located close to an OAR. Figure 4.9 shows CTV delineated in pink next to the heart that is delineated in yellow. The two structures overlap each other, and thereby increase the heart dose.

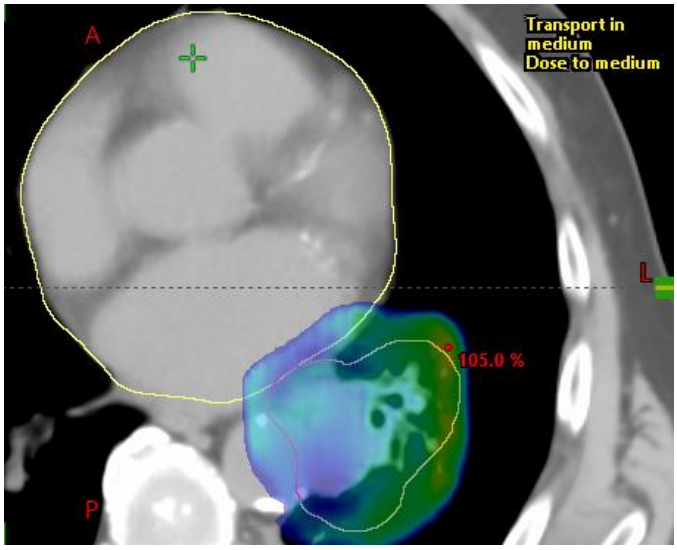

Figure 4.9: Patient 28 had increased heart dose, possibly due to overlap between CTV (pink line) and the patient's heart (yellow line).

The same patient also had some hot spots, and figure 4.10 shows a hot spot (114.9% of the absolute dose) from recalculation week 3. This hot spot was located in the lungs, just outside of the CTV, and resulted in increased dose to the lungs.

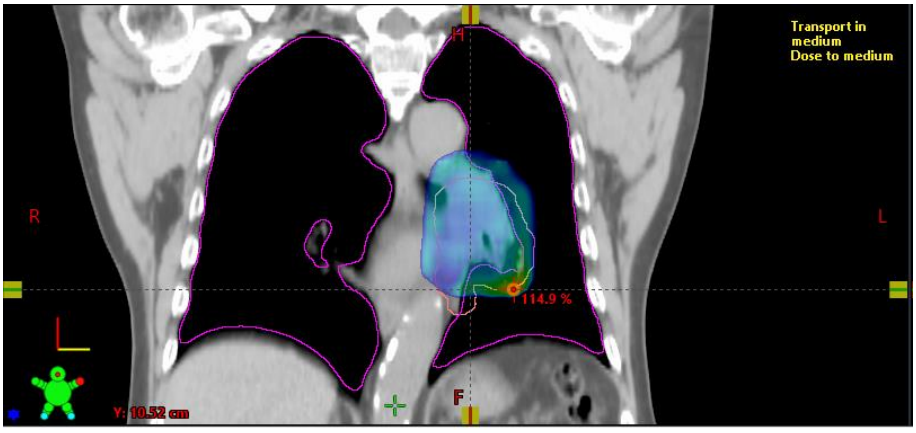

Figure 4.10: Hot spot of patient 28, located in the lungs by 114.9% of the absolute dose.

4.3 Correlation between dosimetric results and the traffic light protocol

This part of the results presents correlations between the traffic light protocol and the dosimetric results found from the recalculations week 1 and week 3. Through this chapter, patients 31 and 34 were excluded. Correlation between V95 CTV from the recalculation and the clinical traffic light colors at the day of the rCT, is plotted in figure 4.11 for week 1 and week 3.

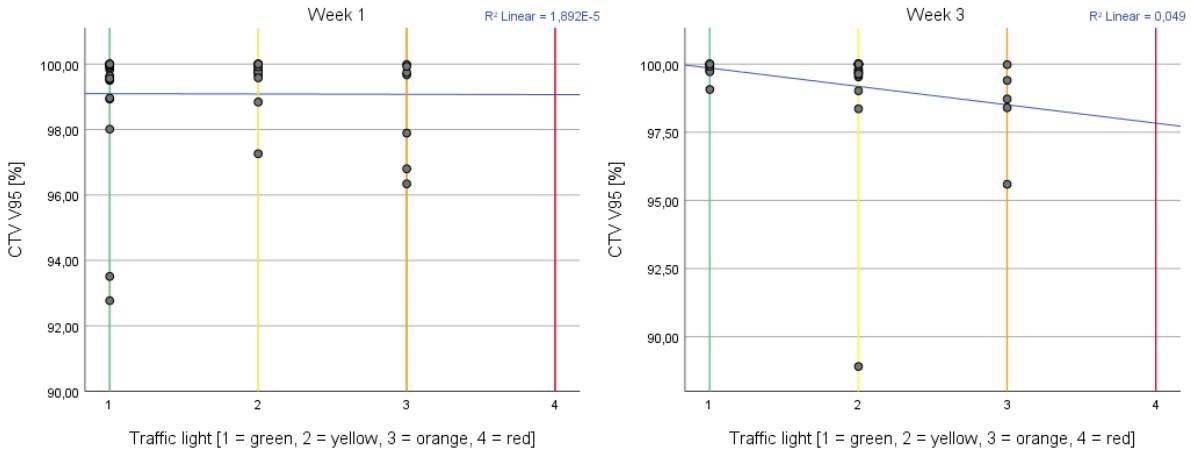

Figure 4.11: Correlation between clinical traffic light color registrations and CTV V95 [%] week 1 and week 3. All possible traffic lights are represented at the x-axis, and CTV V95 [%] values for all patients are represented as dots. The blue line shows the linear regression for V95 as a function of traffic light color, and the R^2 of the regression model is also represented.

The linear regression curve for week 1 is almost straight horizontal (no slope). This indicates that there were no correlations between CTV V95 and traffic light color. Five out of the 12 patients who failed the clinical goal of CTV V95 in week 1 (table 4.5) were assigned the color green. The R-squared value is especially low, which means that there is a small amount (0.000019%) of the data that can be explained by this linear regression curve.

For week 3, the R-squared value indicates that 5% of the data can be explained by the linear regression curve, which has more of a slope. The patients receiving green color from the protocol have higher CTV V95, than for the patients with yellow or orange color. All the

patients who failed CTV V95 in week 3 (table 4.5) received the color yellow or orange, which correlates better with the purpose of the protocol.

The same type of correlation plot, with updated traffic light registrations for the first 19 patients, gives new regression results shown in figure 4.12. $R^2 = 0.132$ week 1, and $R^2 = 0.050$ week 3. The blue line of week 1 is then steeper downwards from green to orange, but the blue line of week 3 is almost unaffected. The R^2-value of week 1 now expresses that 13% of the data can be represented by the linear regression curve. There was a better correlation between CTV V95 and the updated traffic light color registrations after re-evaluation.

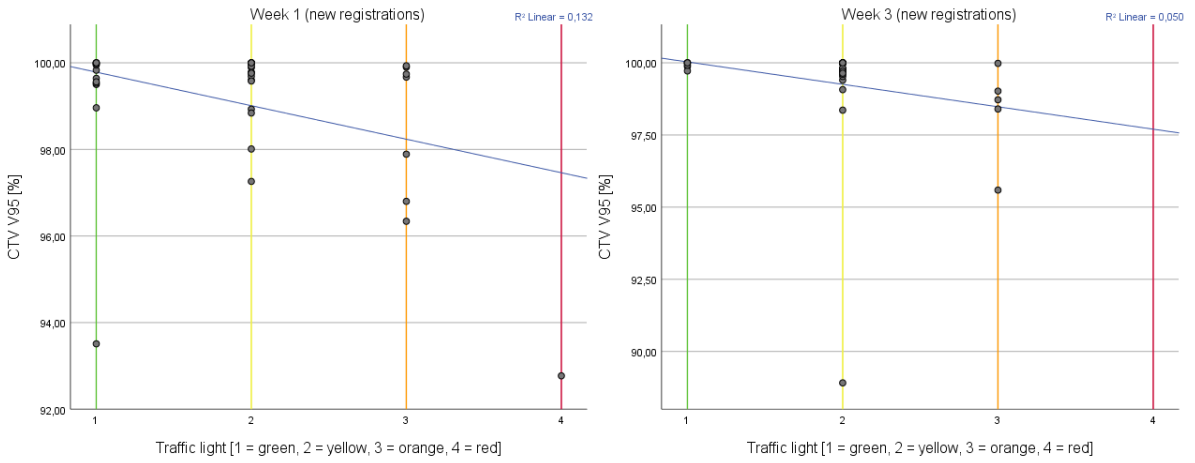

Figure 4.12: Correlation between updated traffic light color registrations (first 19 patients have their registration replaced with the re-evaluated one) and CTV V95 [%] week 1 and week 3. All possible traffic lights are represented at the x-axis, and CTV V95 [%] values for all patients are represented as dots. The blue line shows the linear regression for V95 as a function of traffic light color, and the R^2 of the regression model is also represented.

Correlation between traffic light registrations and other parameters were also plotted, but the re-evaluated registrations were not taken into account for this part. Figure 4.13 illustrates the values of Body D0.1 and which traffic light code all patients received for week 1, and figure 4.14 for week 3. The purple line represents the clinical goal BODY D0.1 cm3 ≤ 107 %, and all the dots above that line are patients who failed the goal.

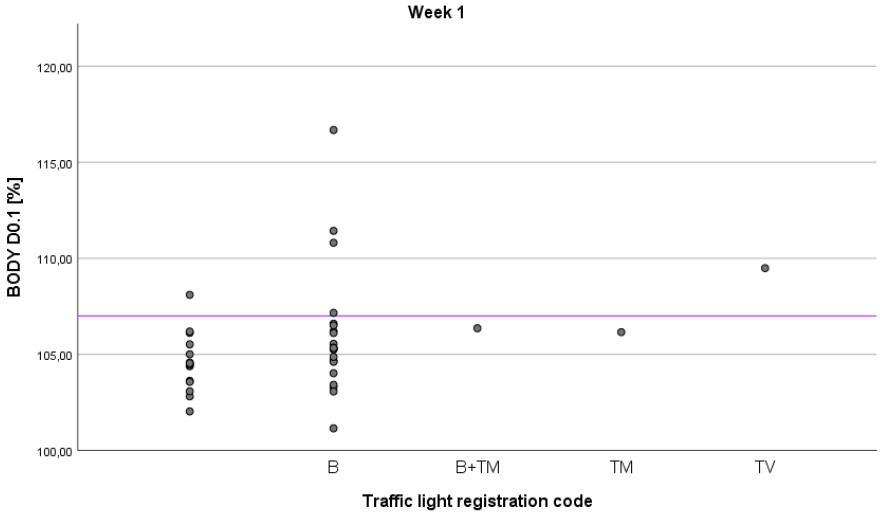

Figure 4.13: Correlation between BODY D0.1 [%] (y-axis) and traffic light registration code (x-axis) week 1. The empty spot on the x-axis is reserved for patients who did not receive any code of anatomical change. The purple line represents the clinical goal of BODY D0.1 $cm^3 \leq 107$ %, and patients above the line failed the goal.

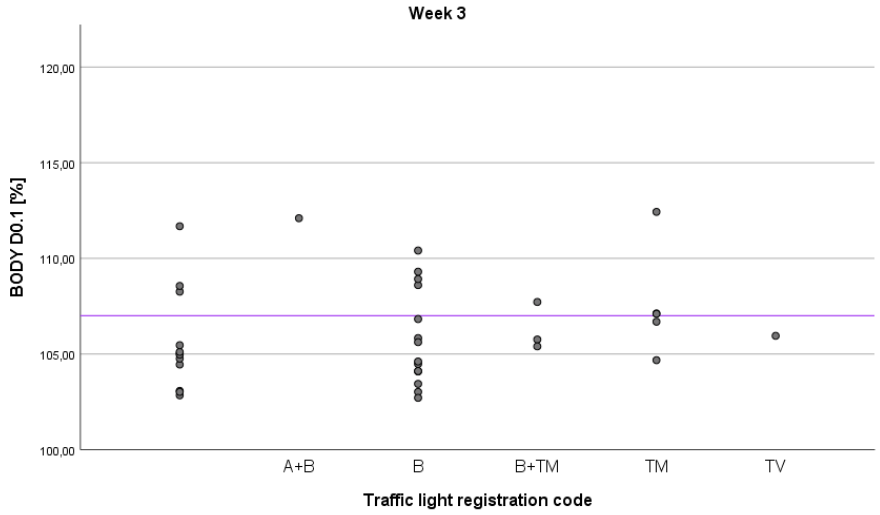

Figure 4.14: Correlation between BODY D0.1 [%] (y-axis) and traffic light registration code (x-axis) week 3. The empty spot on the x-axis is reserved for patients who did not receive any code of anatomical change. The purple line represents the clinical goal of BODY D0.1 $cm^3 \leq 107$ %, and patients above the line failed the goal.

Correlations between Heart D0.1 and traffic light codes are represented in figure 4.15 for week 1, and figure 4.16 for week 3. The blue line represents the clinical goal of Heart D0.1 $cm^3 \leq 66$ Gy, and the dots above the line are patients who failed the goal.

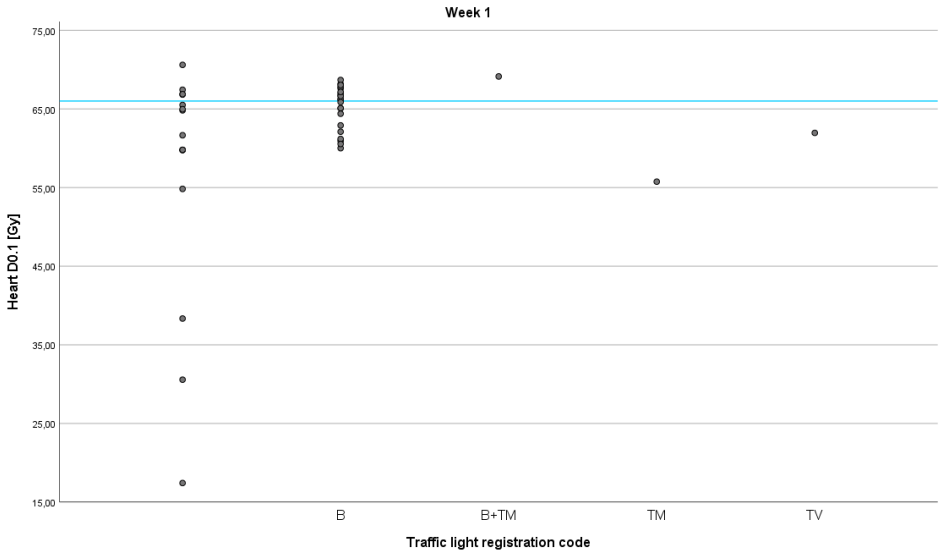

Figure 4.15: Correlation between heart D0.1 [Gy] (y-axis) and traffic light registration code (x-axis) week 1. The empty spot on the x-axis is reserved for patients who did not receive any code of anatomical change. The blue line represents the clinical goal of heart D0.1 $cm^3 \leq 66$ Gy, and patients above the line failed the goal.

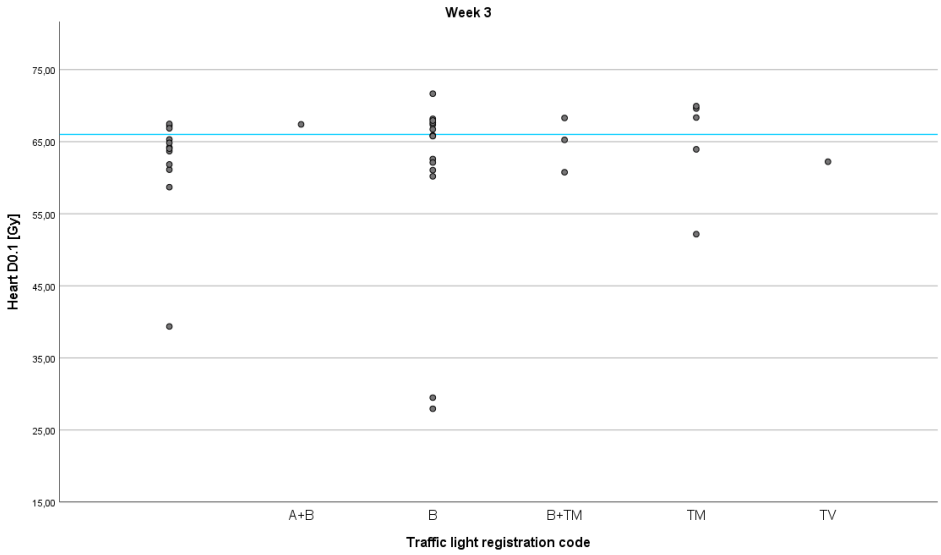

Figure 4.16: Correlation between heart D0.1 [Gy] (y-axis) and traffic light registration code (x-axis) week 1. The empty spot on the x-axis is reserved for patients who did not receive any code of anatomical change. The blue line represents the clinical goal of heart D0.1 $cm^3 \leq 66$ Gy, and patients above the line failed the goal.

Most of the patients who failed the Heart D0.1 goal, were registered with a code of anatomical change, mostly baseline shift. It is worth noting that some patients who failed the goal did not receive any code.

4.4 Estimated delivered dose during treatment

In this chapter, the results from recalculation based on tumor-match are presented. First, some parameters for the tumor-match patients are represented. Figure 4.17 shows CTV V95 for both the bone-match and tumor-match. Some of the patients received tumor-match both weeks, so they are separated by W1 (week 3) and W3 (week 3). The dotted line represents the clinical goal CTV V95% ≥ 99 %.

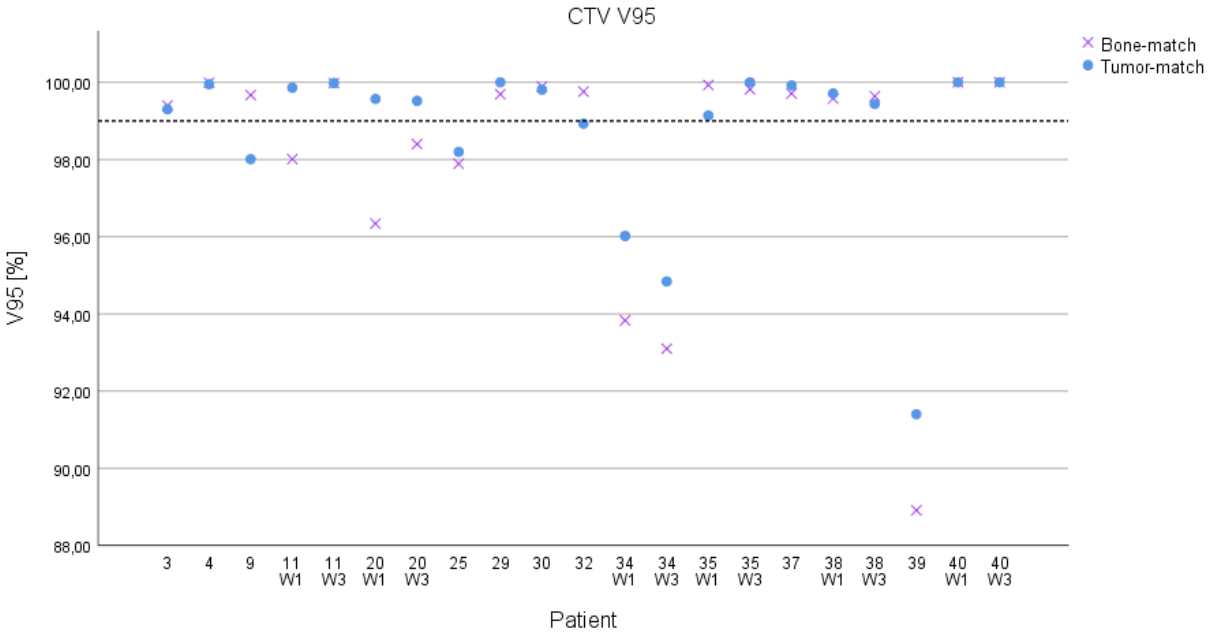

Figure 4.17: CTV V95 [%] differences between bone-match and tumor-match recalculations for the 15 patients who received tumor-match clinically week 1 and/or week 3. Values for bone-match marked by a purple cross, and values for tumor-match marked by blue dots. The black dotted line represents the clinical goal of CTV V95% ≥ 99%.

For most patients the target coverage stayed approximately the same or got better with the tumor-match. The difference was bigger for the patients who had especially poor target coverage, like patient 34 (both weeks) and 39, than for the patients with good target coverage. Patient 11 (week 1) and patient 20 (both weeks) increased the target coverage in such a way that they passed the clinical goal with tumor-matching. Patient 9 resulted in the opposite, from passing to failing, when tumor-match was implemented.

The absolute difference between bone-match and tumor-match were studied for the parameters Body V107, Esophagus D0.1, and heart D0.1. Figure 4.18 illustrates the difference in Body V107 for all patients. The patients plotted above the origin line of zero benefited from the bone-match regarding V107, and the patients below benefited from the tumor-match. Figure 4.19 represents the same type of plot only by Esophagus D0.1, and figure 4.20 represents heart D0.1.

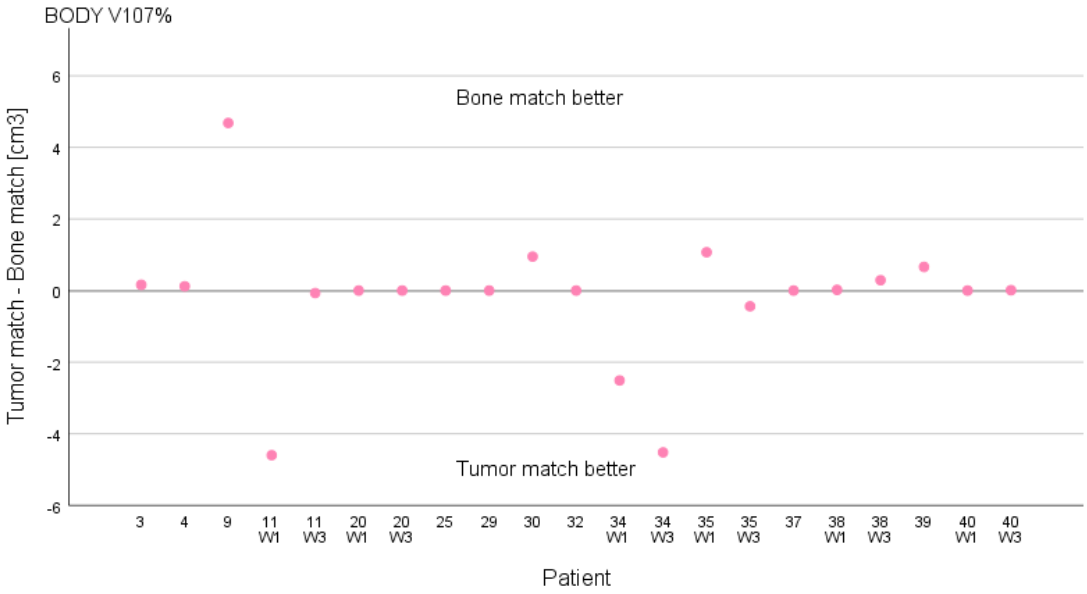

Figure 4.18: The absolute difference [cm^3] between bone-match and tumor-match for Body V107. Each patient represented with a pink dot, and patients located above 0 benefited from bone-match, while patients below 0 benefited from tumor-match.

Most patients had almost the same results for OARs for bone-match and tumor-match, and are thereby close, or equal to zero. Patient 11 (week 1) and 34 (both weeks) had a better outcome from the tumor-match for Body V107, and also received better target coverage (CTV V95) from the tumor-match.

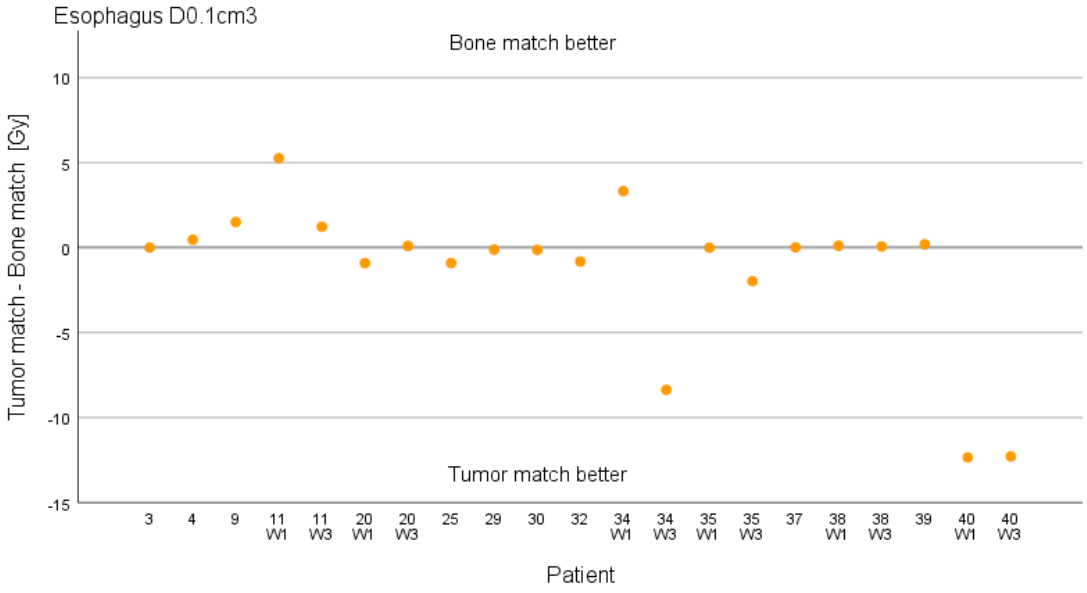

Figure 4.19: The absolute difference [Gy] between bone-match and tumor-match for esophagus D0.1 cm^3. Each patient represented with an orange dot, and patients located above 0 benefited from bone-match, while patients below 0 benefited from tumor-match.

Patient 11 benefited from the bone-match for Esophagus D0.1, and patient 34 benefited from bone-match only week 1 and not week 3. Patient 40 (both weeks), who had good target coverage for both matches, had the biggest difference in Esophagus D0.1. Tumor-match was more dose sparing for the esophagus for this patient, but both matches were below the constraints of 66 Gy.

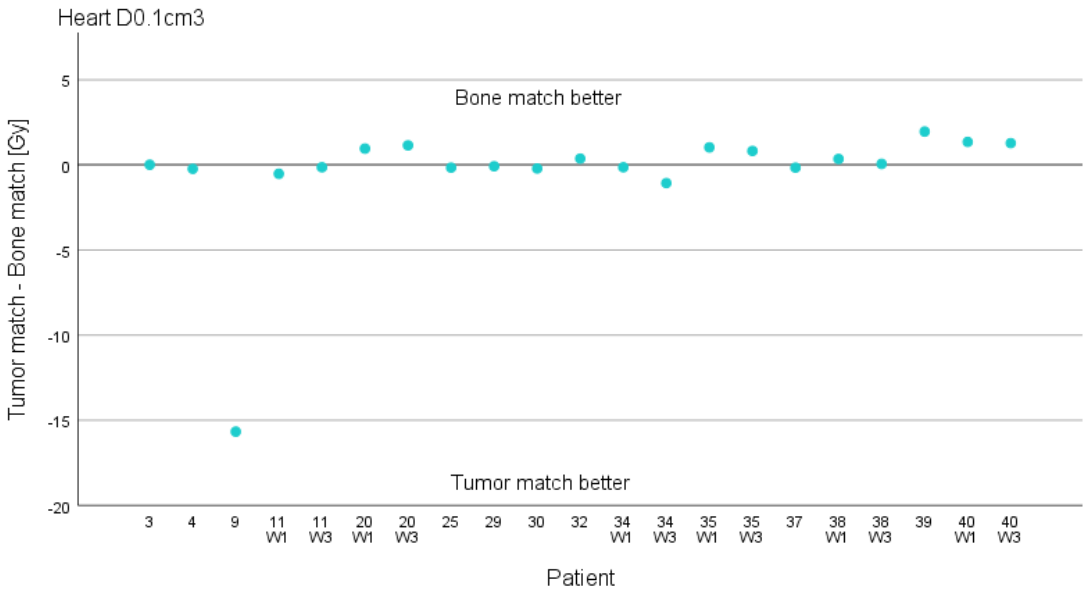

Figure 4.20: The absolute difference [Gy] between bone-match and tumor-match for heart D0.1 cm^3. Each patient represented with a blue dot, and patients located above 0 benefited from bone-match, while patients below 0 benefited from tumor-match.

There was not a significant difference between CTV V95 for all 41 patients, whether tumor-matching was present or not for the 15 patients who received it clinically ($p = 0.346$ by Friedman's ANOVA test). The null hypothesis that the estimated clinical target cover is the same as the estimated target coverage sticking to bone-match, was retained.

In evaluation of these estimated clinical results, it was in summation an increase of one CTV V95 parameter above the goal, compared to the bone alignment results (bone-match for all patients). In summation of body V107, one more recalculated plan failed the associated goal. Esophagus D0.1cm^3 and Heart D0.1cm^3 both had zero change in recalculated plans above or under their associated goals.

5. Discussion

Dosimetric results for bone alignment.

The median value first decreases in week 1 and increases slightly again at week 3, for both CTV V95 and D98. Both changed significantly during these first three weeks of treatment, so CTV coverage was significantly better in planning, compared to the week 1 and week 3 plan. When the patient's anatomy changes, the tissue density differs, and the photon beam attenuates differently. In general, poorer CTV coverage is probably due to this, but other reasons will be discussed later. Also, the longer between the CT scans, the more time to develop anatomical changes. It could take up to a week between the pCT and the start of the treatment, and this might explain the significant change between planning and week 1 for D98 and V95. There was not a significant difference in CTV coverage from week 1 to week 3, even though the time gap between them was most likely bigger than between planning and week 1.

Of the recalculated treatment plans, 19/79 failed the clinical goal of CTV V95 (table 4.5). There were multiple other clinical goal failures of OARs, especially for heart and esophagus. 32 patients failed D0.1 for the heart.

Traffic light protocol

The study by Kwint et al. [46] showed that most ITACs (or anatomical changes) occurred during the first week of treatment, and then decayed further during the treatment course. Our data is not quite in agreement with this since there were more codes of anatomical changes present week 3 than for week 1. An increase of tumor regression was the biggest difference in registered codes from week 1 – week 3. Also, three of the patients did not get a registration in week 3, it could be reported more codes of anatomical changes week 3 if these patients were present. An increase of tumor regression reports is natural, and in fact what we want to achieve. For Kwint et al. [46] patients, most cases of tumor regression were also observed in week 3. Even though there were more anatomical changes present week 3 for our patients, the CTV coverage had no significant change between week 1 and week 3. Tumor regression does not necessarily result in poorer CTV coverage but could result in increased dose to other healthy tissue.

Baseline shift were the most present anatomical change for the 41 patients in this thesis (73.2% of the patients). For Kwint et al. [46] patients, baseline shift was observed for 32% of their 177 patients. Also, more CBCTs over the treatment course were present in that study compared to this thesis. It is worth noticing that there were no observations of pleural effusion and infiltrative changes, only one observation of atelectasis, and one of tumor progression, for our patients. Our data is cross-sectional, but to include the rest of the protocol registrations was beyond the scope of this thesis. The cross-sectional data included are assumed to be representative enough, and it is still interesting to discuss why there is a small variation of anatomical change codes represented for our patients.

Re-evaluation

The re-evaluation of the first 19 patients shows that almost half of the traffic light registrations were possibly wrongly evaluated to some degree. Most of the color registrations that changed, changed into a color representing a worse degree of anatomical change. The biggest contrast between the old and new registrations, were patient 16 that should be evaluated as red but received green clinically. The week 1 rCT was taken the same day as fraction 2 for this patient. Fortunately, the patient's tumor progression was detected right after fraction 4 was delivered, and from fraction 5 a replan was used. But the fact that this patient received the fractions, when the traffic light registration was supposed to be red, is quite critical and contrary to the protocol.

The 12 additional registrations of anatomical change for the re-evaluation, is an indication that these patients may have been underreported. The re-evaluated registrations resulted in a better correlation with CTV V95 as figure 4.12 shows, compared to the clinical registrations of figure 4.11. This indicates that a training phase of CBCT evaluation for RTTs pays off, and gives traffic light registrations that correlates better with the patients target coverage and need of adaptations. The R^2 still indicates that a lower amount of the data can be expressed by the linear regression curve. The red registration (patient 16) of week 3 contributes to the steeper regression line in figure 4.12. That patient's re-evaluation from green to red, results in one less green registration with low value of CTV V95.

The re-evaluated results are a better representation of how well the protocol worked, since the CBCT were studied by the most experienced RTT at the clinic. In this way, it can represent the well-functioning of the protocol for trained RTTs. As figure 4.11 (the clinical registrations) shows, the registrations of week 3 has better correlation than week 1. Almost all patients who received green color had CTV V95 close to 99%. This emphasizes the learning curve of the protocol.

Of the failed CTV V95, 17/19 were detected by the protocol and registered as yellow, orange, or red (after re-evaluation). This means that the protocol detected poor target coverage in most cases. However, of yellow and orange registrations, 43 did not indicate poor CTV coverage from the recalculations. The majority of these patients failed a clinical goal of one or multiple OARs, on the other hand.

Replan

Sixteen patients (9%) required an adapted treatment plan as a result from the anatomical changes in Kwint et al. [46] study. In our study, five patients (12.2%) received a replan clinically between week 1 and week 3. Møller et al. [51] study also resulted in replan for 12% of the patients, with 163 patients present compared to our 41 patients. Atelectasis was present for 85% adaptive treatment plans in Møller et al. study. There was no pattern of anatomical change that triggered replan clinically for the five patients in this thesis, in comparison.

As mentioned, baseline shift was the most common anatomical change present for our patients, and orange color was triggered by a shift of 5 mm. Møller et al. had the same trigger criteria for the shift to have expected geometric effect on target coverage, also measured based on bone-match. Compared to our 73.2% presence of baseline shift, only 9% (N=14) of Møller et al. patients experienced it. Most of them had atelectasis causing the shift, but for our patients' atelectasis was only registered once. The difference in baseline shift and atelectasis registrations might be due to different training of RTTs. Detection of atelectasis is difficult since the presence can be quite vague on the CBCT. Anatomical changes like tumor progression and regression were not evaluated in Møller et al study.

It is complex to evaluate if the replans were based on reasonable decisions, and if it resulted in a better treatment. The evaluation could be done by studying dosimetric differences between week 1 and week 3, since all replans were implemented in between the two rCTs. For example, patient 16 had an increase of CTV V95 from week 1 (92.8%) to week 3 (98.7%), but at the same time mean dose for esophagus increased from week 1 (29.7 Gy) to week 3 (35.9 Gy). So, the replan resulted in a better target coverage, but the esophagus received a drastically higher dose. Patient 25 increased CTV D98 from week 1 (94.8%) to week 3 (99.5%), which was an excellent upgrade. At the same time the patient went from failing clinical goals of esophagus and heart week 1, to failing clinical goals of body and lungs week 3.

In another study by Møller et al. [56], they also evaluated the effect of ART for advanced lung cancer. The study had different trigger criteria and not a traffic light protocol like our study, but 79 adaptations were performed. Twenty of the adaptations obtained no gain in target coverage or correction of spinal cord dosage, and 16 of them were not justifiable. As mentioned, to evaluate if our replans were justifiable is complex and depends on what would be the criteria for such a statement, when looking at examples like patient 16 and 25. Of the four replans made based on anatomical changes (one was bound to technical issues), none gained target coverage without jeopardizing healthy tissue according to the week 3 recalculation.

Of the patients not adapted in Møller et al. [56] study, a recalculation process similar to ours resulted in only one patient who slipped through their adaptation trigger criteria. When studying the week 1 target coverage for all our patients, patient 20, 31, 34 had the most critical results. Patients 31 (V95=89.8%) and 34 (V95=93.8%) should probably have received a replan when looking at the responsible oncologist's delineation (where these parameters are drawn from). On the other hand, the decision of adaptations was made from the pCT which had delineation following old requirements and is thereby not possible to discuss further in this thesis. Patient 20 had anatomical changes of orange color discovered by the protocol. The evaluation of a replan was then present clinically, but tumor-match treatment was concluded as the solution to ensure target coverage. For this patient the tumor-match treatment gave a CTV V95 increase from 96.3% to 99.5%. Replan was not necessary to improve target coverage when tumor-match were present. Tumor-match will be discussed more later.

There were patients that had sufficient target coverage week 1 but failed clinical goals of OAR, like patient 30 resulted in body V107 = 16.9 cm^3 (the highest outliner of figure 4.5). This is an extremely high value, but the rest of the clinical goals were not equally as bad. The patient received yellow + tumor regression from the protocol, so clinically they were might aware of risks but did not decide a replan or tumor-match treatment. Based on our recalculation, this patient could have been a candidate for adaptation because of hot spots, but the worst hot spot (114.8%) was located inside the CTV. The occurrence of hot spots varies in general for the patients in this study, and it was shown a significant difference in body V107 between planning, week 1 and week 3. Hot spots were not further investigated. Hot spots might be accepted for tumor sites like small tumors in the lungs, but in general they are considered undesirable [59]. Hot spots can cause critical consequences for the organs it is present for, but as long as it is not present in each fraction it is not that harmful.

Correlations

This part will discuss correlation between the clinical registrations and dosimetric results, even though the re-evaluation was more representative for the registrations. Challenges of CBCT evaluation will be discussed.

Figure 4.4 shows that the two worst cases of CTV D98 are patients 31 and 34 who were excluded from the correlation analysis due to the irregular delineation. The rest of the patients participated in correlation between the traffic light protocol and dosimetric results from bone alignment. It is interesting to note, that even though the target cover did not change significantly from week 1 to week 3, the yellow traffic light registrations increased, and the green registrations decreased.

Ideally the V95 values of figure 4.11 would be high for the green traffic light registration, and decay further for the other colors. For week 1, patients 16 and 39 scored less than 94% for CTV V95, and they were not detected by the protocol (registered as green). Patient 16 were detected with re-evaluation. Patient 39 was scoring less than 90% week 3, but at least this time the patient was registered as yellow and received tumor-match treatment. The reason for the bad correlation between traffic light color and target coverage is probably that some anatomical changes were not detected by the inspection of the CBCTs. As discussed, a learning curve was present.

Structures are not delineated on the CBCT, and to observe changes can be challenging when comparing the pCT with the daily CBCT. Studying the rCT and pCT past treatment, the delineation by the oncologist is present, and the two scans have the same image quality. These two factors make it easier to detect anatomical changes, such as baseline shift. There is no time to get delineations of CBCTs for on-line ART, and the traffic light registrations must be made within a certain time frame. The tumor progression of patient 16, might not have been discovered if it were not for the rCTs implementation connected to the pulmDIBH study.

When studying body D0.1 and heart D0.1 parameters compared to traffic light code (figure 4.13, 4.14, 4.15, and 4.16), there were some patients who failed the clinical goal and also did not receive a code. Ideally, the patients failing heart D0.1, would have a code representing an underlying cause. On the other hand, a color registration without a code could represent the anatomical change causing the clinical goal failure. There are patients that received yellow or orange color without an associated code in this thesis, but these are not the patients without code of figure 4.13, 4.14, 4.15, and 4.16. All patients who failed the body and heart D0.1 goals, that did not receive code of anatomical change, were registered with the color green (i.e these patients were not detected by the traffic light protocol). Have in mind that these code registrations were not the re-evaluated ones, and the re-evaluated had more codes present. This could have made an impact on these results, e.g that more patients who failed the clinical goals received codes of anatomical change.

Passing the clinical goal of body D0.1 and heart D0.1 and still receiving a code, can have a natural cause. The anatomical change present could affect the target coverage or other OARs than body and heart. Correlations between the presence of codes and other structures were beyond the scope of this thesis but would be interesting to investigate further. The traffic light protocol did not correlate to OAR, which was expected since the protocol only evaluates the geometric view and no values of dosage.

Errors in general

Patients that failed clinical goal(s), were might not detected by the protocol for logical reasons. Anatomical changes that caused a slight increase above constraints, could have been hard to detect on the CBCT. Another reason is that the patient setup of rCT and CBCT could differ, since the CT machines were in two different rooms and the patient had to move. It could also have been some waiting time between the two scans that could have affected the CT scans. The rCT recalculation was only an estimate of the treatment given clinically. The rCT could have a different breathing level than for the pCT, but also the treatment delivery itself.

The image registration by the candidate involved some possibility of errors that could affect the recalculations and is a simple explanation of small clinical goal failures in general. Møller et al. [51] used CBCT to correct setup error of the bone anatomy with a region of interest that included the spine. HUH traffic light protocol and the pulmDIBH study also used bone anatomy for patient setup, and our image registrations also prioritized the spine.

Tumor-match patients and the estimated delivered dose during treatment

There are a lot to consider when evaluating the tumor-match versus bone-match treatments. Firstly, the target coverage should be improved. For most of our patients, it was improved or stayed approximately the same, as figure 4.17 shows. In total, 5/21 recalculated tumor-match plans resulted in better CTV V95 with an increase of 1% or more.

Patient 20, who was represented as a patient case earlier, had improved target coverage for both weeks (from below to above constraints). Improvement of target coverage did not necessarily mean that the tumor-match was better. The OARs needed to be evaluated, as the tumor-match should not have negative consequences for OAR doses. Studying heart D0.1, patient 20 would benefit more of a bone-match treatment. On the other hand, heart D0.1 were below constraints for both matches. Tumor-match improved heart D0.1 for patient 9 drastically, while target coverage went from above to below constraints and body V107 went from below to above constraints. But again, the bone-match already passed the clinical goal of heart D0.1. Improving an already sufficient heart dose while sacrificing the target dose and healthy tissue might not be justified. The most important part of ART is to ensure target coverage. After evaluation of body, esophagus, and heart, it is assumed that 4/21 tumor-match treatments were beneficial.

Nyeng [60] researched the dosimetric impact from soft tissue matching on 35 NSCLC patients. It resulted in significant reduction of the PTV volumes, and average mean lung dose then reduced by 2.1 Gy. There were no significant changes in doses to the heart, esophagus, and spinal cord. The risk of severe radiation pneumonitis may be reduced by decreasing the lung dose. For our data, the average D0.1 lungs was reduced by 0.6 Gy, the average D0.1 heart was reduced by 0.4 Gy, and the average D0.1 esophagus was reduced by 1.2 Gy, when changing from bone-match to tumor-match. The biggest contribution to the reduction of D0.1 esophagus was patient 40, as seen in figure 4.19. The isocenter was located further away from esophagus with tumor-match for this patient.

Margins, like PTV margin, can be reduced by ART and on-line soft tissue match, and it improves precision in radiation therapy [61]. Møller et al. [4] study decreased mean PTV volumes from 456 cm^3 to 270 cm^3 when introducing tumor-match and ART for NSCLC patients. The study resulted in reduction of irradiated volumes of heart and lungs, while maintaining loco-regional control. For our protocol and study, tumor-match was only a possibility connected to the protocol, but was not used for all patients. The traffic light registrations were made by bone-matching, and the same goes for Kwint et al. [46] patients. Maybe it is possible to make a new version of the traffic light protocol based on tumor-match only, like Møller et al [4]. At the same time, bone-match is safer when it comes to doses to OARs as long as the protocol is off-line ART. As the protocol stands today, there was not a big part that gained much from the tumor-match. Then again, the patients with the worst target coverage (like patient 34 and 39) gained the most from the tumor-match, but still not sufficient in relation to the clinical goal.

Having the choice of tumor-match as part of the protocol, gave no significant impact on the target coverage for our patients. This contradicts other studies. As seen, there were some patients present in our study that benefited from the tumor-match, like patient 20. If it was not for the tumor-match, the patient might need a replan, which would be more time consuming.

A well-functioning ART, with evaluation of soft-tissue CBCT match, requires correct training of RTTs [61]. As discussed earlier, evaluation of CBCT scans can be difficult, especially for detecting certain anatomical changes. It is worth mentioning that there could be a lack of information in the protocol register available for the candidate. Patients could receive tumor-match but not have it registered.

Future work

These patients could benefit from on-line adaptation, like treatment by the Ethos machine. A retrospective study using an Ethos Emulator was done by Mao et al. [62] and included 297 fractions distributed among ten patients with LA lung cancer (9 of them with NSCLC). The on-line treatment by Ethos ensures OAR doses, as well as target coverage, with automatic contouring of CBCT images and dose distributions optimized based on the daily CBCT. The study resulted in improved target coverage and normal tissue sparing by 3.3% for the automated ART. The accuracy of automatic contouring by Ethos was considered clinically acceptable for these patients.

Artificial intelligence (AI) techniques could also be used to improve CBCT image quality in less than a second once a model is trained, as shown from Zhang et al. [63] study. The result of the study implies that the improved CBCT can be close to the image quality of conventional CT, and has potential for adaptive planning. If the quality improvement could be used for off-line adaptation, e.g our traffic light protocol, it would be interesting to see if it could be helpful for the RTTs when evaluating the CBCTs. Recalculation performed on CBCT scans would also be more successful and feasible if the image quality was better.

In 2025, modern proton therapy will be available in Norway, and could be a treatment alternative for these patients. It allows substantial reduction of dose and toxicity of OARs such as lungs, heart, and spinal canal [64]. There are multiple ongoing clinical studies, in both USA and Europe, investigating the potential of modern proton therapy (clinicalTrials.org: NCT02731001, NCT01629498, NCT01993810). An adaptive strategy will still be important for proton therapy. How well the traffic light protocol would work with proton therapy, would need evaluation. As Hoffmann et al. [55] study showed, proton therapy had a more crucial need of adaptations compared to photon therapy.

6. Conclusion

In this thesis the impact from anatomical changes for LA-NSCLC was studied, with an evaluation of HUH traffic light protocol for detection of these changes. Treatment plan recalculation on CT scans for the first and third week of treatment, resulted in significant change of target coverage (CTV V95) during these weeks, and 19/79 recalculations failed the clinical goal of CTV V95 % $\geq$ 99 %. A noticeable part of the recalculations resulted in clinical goal failure for OARs, e.g 32 failures for D0.1 heart.

The re-evaluation of the traffic light registrations resulted in correlation between the registrations and target coverage. This showed that protocol training has influence on the identification of the patients with anatomical changes. Of the failed CTV V95 from the recalculations, 17/19 received a color of yellow, orange or red. Several patients who failed clinical goals of heart and/or body, received a green color registration with no anatomical change reported. There was no clear correlation between the protocol registrations and OARs, which was however expected. All patients that failed D0.1 clinical goals of body and heart, and also did not receive a code of anatomical changes, were registered as green. This could motivate on-line adaptation for these patients.

There were different triggers for the replan decisions made by the radiation therapy therapist. Recalculations of the replans resulted in better target coverage, but at the same time healthy tissue and OARs were affected by higher doses for all replans. For the patients evaluated for tumor-match treatment, the target coverage was not significantly improved, in contrast to other studies. Only 4/21 tumor-match treatments were beneficial, when dosimetric results of body, heart, and esophagus were taken into account.

Treating the thorax area is challenging, and there are several uncertainties in our results. An effective adaptive protocol is essential for treatment of LA-NSCLC, and further research is important. Our traffic light protocol detects patients expecting low target coverage, but OARs are too complex to evaluate by our protocol. On-line adaptation could be a solution, but the protocol has potential and needs further investigation.

Bibliography

[1] Sung H, Ferlay J, Siegel RL, Laversanne M, Soerjomataram I, Jemal A, et al. Global Cancer Statistics 2020: GLOBOCAN Estimates of Incidence and Mortality Worldwide for 36 Cancers in 185 Countries. CA Cancer J Clin. 2021;71(3):209-49.

[2] KVIST-group. Professional guidelines for curative radiotherapy of non-small cell lung cancer. Norway; 2017.

[3] Helsedirektoratet. Nasjonalt handlingsprogram med retningslinjer for diagnostikk, behandling og oppfølging av lungekreft, mesoteliom og thymom. 2013.

[4] Møller DS, Lutz CM, Khalil AA, Alber M, Holt MI, Kandi M, et al. Survival benefits for non-small cell lung cancer patients treated with adaptive radiotherapy. Radiother Oncol. 2022;168:234-40.

[5] Non-Small Cell Lung Cancer Treatment (PDQ®)–Patient Version Cancer.gov: National Cancer Institute; [updated 27.08.2021. Available from: https://www.cancer.gov/types/lung/patient/non-small-cell-lung-treatment-pdq.

[6] Peracchia C, Anaizi NH. Lung Function in Health and Disease : Basic Concepts of Respiratory Physiology and Pathophysiology: Bentham Science Publishers; 2014.

[7] Ganti AK, Gerber DE. Lung Cancer. Cary, UNITED STATES: Oxford University Press, Incorporated; 2013.

[8] Bast RC. Holland-Frei cancer medicine. Hoboken, New Jersey: Wiley Blackwell; 2017.

[9] Cancer Registry of Norway. Lungekreft Cancer Registry of Norway: Institute of populationbased cancer research [updated 02.11.2022; cited 2023 20.01]. Available from: https://www.kreftregisteret.no/Temasider/kreftformer/Lungekreft/.

[10] Duma N, Santana-Davila R, Molina JR. Non-Small Cell Lung Cancer: Epidemiology, Screening, Diagnosis, and Treatment. Mayo Clinic proceedings. 2019;94(8):1623-40.

[11] What you need to know about small cell lung cancer LUNGevity.org: LUNGevity; 2020 [Available from: https://www.lungevity.org/sites/default/files/request-materials/LUNGevity-SCLC-booklet-110920.pdf.

[12] European Health Union: A new EU approach on cancer detection – screening more and screening better [press release]. Brussels2022.

[13] Lung cancer screenings to begin in Norway Norwegian Cancer Society2020 [Norwegian Cancer Society. Available from: https://kreftforeningen.no/en/lung-cancer-screenings-to-begin-in-norway/.

[14] Non-Small Cell Lung Cancer Treatment (PDQ®)–Health Professional Version Cancer.gov: National Cancer Institute; [updated 17.02.2023. Available from: https://www.cancer.gov/types/lung/hp/non-small-cell-lung-treatment-pdq.

[15] Radiation Oncology Physics. Vienna: INTERNATIONAL ATOMIC ENERGY AGENCY; 2005.

[16] Hall EJ, Giaccia AJ. Radiobiology for the radiologist. Philadelphia: Wolters Kluwer; 2019.

[17] What you need to know about stage III non-small cell lung cancer Lungevity.org: Lungevity; 2022 [Available from: https://www.lungevity.org/for-patients-caregivers/helpful-resources/get-educational-materials.

[18] O'Sullivan B, Brierley J, Byrd D, Bosman F, Kehoe S, Kossary C, et al. The TNM classification of malignant tumours—towards common understanding and reasonable expectations. Lancet Oncol. 2017;18(7):849-51.

[19] Brierley JD, Gospodarowicz MK, Wittekind C. Lung, Pleural, and Thymic Tumours. United Kingdom: United Kingdom: John Wiley & Sons, Incorporated; 2017.

[20] Cancer Registry of Norway. Cancer in Norway 2021 - Cancer incidence, mortality, survival and prevalence in Norway2022:[113 p.]. Available from: https://www.kreftregisteret.no/globalassets/cancer-in-norway/2021/cin_report.pdf.
[21] Spigel DR, Faivre-Finn C, Gray JE, Vicente D, Planchard D, Paz-Ares L, et al. Five-Year Survival Outcomes From the PACIFIC Trial: Durvalumab After Chemoradiotherapy in Stage III Non-Small-Cell Lung Cancer. J Clin Oncol. 2022;40(12):1301-11.
[22] Joiner M, Kogel Avd, editors. Basic Clinical Radiobiology. 4 ed. London: Hodder Arnold; 2009.
[23] Radiation Therapy to Treat Cancer Cancer.gov: National Cancer Institute; [updated 08.01.2019. Available from: https://www.cancer.gov/about-cancer/treatment/types/radiation-therapy.
[24] Mayles P, Nahum A, Rosenwald JC. Handbook of radiotherapy physics: Taylor & Francis Group; 2007.
[25] Saha GB. Physics and radiobiology of nuclear medicine. New York: Springer; 2013.
[26] Gibbons JP. Khan's the physics of radiation therapy. Sixth ed. Philadelphia: Lippincott Williams & Wilkins; 2020.
[27] Chalmers AJ, Carruthers RD. Radiobiology Summaries: DNA Damage and Repair. Clin Oncol (R Coll Radiol). 2021;33(5):275-8.
[28] Rowan S, Fisher DE. Mechanisms of apoptotic cell death. Leukemia. 1997;11(4):457-65.
[29] Chang DS. Basic radiotherapy physics and biology. Cham, Switzerland: Springer; 2021.
[30] McWilliam A, Abravan A, Banfill K, Faivre-Finn C, van Herk M. Demystifying the Results of RTOG 0617: Identification of Dose Sensitive Cardiac Subregions Associated With Overall Survival. J Thorac Oncol. 2023;18(5):599-607.
[31] Thames HD. On the origin of dose fractionation regimens in radiotherapy. Seminars in radiation oncology. 1992;2(1):3-9.
[32] Khan FM, Gerbi BJ. Treatment planning in radiation oncology. Philadelphia: Wolters Kluwer/Lippincott Williams & Wilkins Health; 2012.
[33] Thorwarth D. Functional imaging for radiotherapy treatment planning: current status and future directions-a review. Br J Radiol. 2015;88(1051):20150056-.
[34] ICRU. Prescribing, Recording, and Reporting Photon Beam Therapy. U.S.A: International commission on radiation units and measurements; 1993. Report No.: 50.
[35] Nestle U, De Ruysscher D, Ricardi U, Geets X, Belderbos J, Pöttgen C, et al. ESTRO ACROP guidelines for target volume definition in the treatment of locally advanced non-small cell lung cancer. Radiother Oncol. 2018;127(1):1-5.
[36] Lee NY, Riaz N, Lu JJ. Target Volume Delineation for Conformal and Intensity-Modulated Radiation Therapy. Cham: Springer International Publishing : Imprint: Springer; 2015.
[37] Schlegel WC, Bortfeld T, Grosu AL. New Technologies in Radiation Oncology. Berlin, Heidelberg: Springer Berlin Heidelberg : Imprint: Springer; 2006.
[38] Kong M, Hong SE. Comparison of survival rates between 3D conformal radiotherapy and intensity-modulated radiotherapy in patients with stage III non-small cell lung cancer. Onco Targets Ther. 2016;9:7227-34.
[39] Mell LK, Mehrotra AK, Mundt AJ. Intensity-modulated radiation therapy use in the U.S., 2004. Cancer. 2005;104(6):1296-303.
[40] Levernes SG. Volum og doser i ekstern stråleterapi : definisjoner og anbefalinger. Østerås: Statens strålevern; 2012.

[41] Popescu CCMS, Olivotto IAMD, Beckham WAPD, Ansbacher WPD, Zavgorodni SPD, Shaffer RFRCP, et al. Volumetric Modulated Arc Therapy Improves Dosimetry and Reduces Treatment Time Compared to Conventional Intensity-Modulated Radiotherapy for Locoregional Radiotherapy of Left-Sided Breast Cancer and Internal Mammary Nodes. Int J Radiat Oncol Biol Phys. 2010;76(1):287-95.
[42] The International Commission on Radiation Units and Measurements. Journal of the ICRU. 2010;10(1).
[43] Klein EE, Hanley J, Bayouth J, Yin F-F, Simon W, Dresser S, et al. Task Group 142 report: Quality assurance of medical accelerators. Med Phys. 2009;36(9):4197-212.
[44] Selvaraj J, Uzan J, Baker C, Nahum A. 4D radiobiological modelling of the interplay effect in conventionally and hypofractionated lung tumour IMRT. Br J Radiol. 2015;88(1045):20140372-.
[45] Chen M, Yang J, Liao Z, Chen J, Xu C, He X, et al. Anatomic change over the course of treatment for non-small cell lung cancer patients and its impact on intensity-modulated radiation therapy and passive-scattering proton therapy deliveries. Radiat Oncol. 2020;15(1):55-.
[46] Kwint M, Conijn S, Schaake E, Knegjens J, Rossi M, Remeijer P, et al. Intra thoracic anatomical changes in lung cancer patients during the course of radiotherapy. Radiother Oncol. 2014;113(3):392-7.
[47] Peroni DG, Boner AL. Atelectasis: mechanisms, diagnosis and management. Paediatr Respir Rev. 2000;1(3):274-8.
[48] Karkhanis VS, Joshi JM. Pleural effusion: diagnosis, treatment, and management. Open Access Emerg Med. 2012;4(default):31-52.
[49] Prunaretty J, Boisselier P, Aillères N, Riou O, Simeon S, Bedos L, et al. Tracking, gating, free-breathing, which technique to use for lung stereotactic treatments? A dosimetric comparison. Rep Pract Oncol Radiother. 2019;24(1):97-104.
[50] Kubo HD, Wang L. Introduction of audio gating to further reduce organ motion in breathing synchronized radiotherapy. Med Phys. 2002;29(3):345-50.
[51] Moller DS, Khalil AA, Knap MM, Hoffmann L. Adaptive radiotherapy of lung cancer patients with pleural effusion or atelectasis. Radiother Oncol. 2014;110(3):517-22.
[52] Yan D, Vicini F, Wong J, Martinez A. Adaptive radiation therapy. Phys Med Biol. 1997;42(1):123-32.
[53] Green OL, Henke LE, Hugo GD. Practical Clinical Workflows for Online and Offline Adaptive Radiation Therapy. Semin Radiat Oncol. 2019;29(3):219-27.
[54] Ragnvaldsen V, Pettersen HES, Fjellanger K, Hysing LB, Redalen KR. Feasibility of Water Equivalent Path Length Analysis in Adaptive Proton Therapy of Locally Advanced Non-Small Cell Lung Cancer. NTNU; 2022.
[55] Hoffmann L, Alber M, Jensen MF, Holt MI, Møller DS. Adaptation is mandatory for intensity modulated proton therapy of advanced lung cancer to ensure target coverage. Radiother Oncol. 2017;122(3):400-5.
[56] Møller DS, Holt MI, Alber M, Tvilum M, Khalil AA, Knap MM, et al. Adaptive radiotherapy for advanced lung cancer ensures target coverage and decreases lung dose. Radiother Oncol. 2016;121(1):32-8.
[57] MacFarland TW, Yates JM. Introduction to Nonparametric Statistics for the Biological Sciences Using R. Cham: Springer International Publishing : Imprint: Springer; 2016.
[58] Armstrong RA. When to use the Bonferroni correction. Ophthalmic Physiol Opt. 2014;34(5):502-8.
[59] Liu W, Zhang X, Li Y, Mohan R. Robust optimization of intensity modulated proton therapy. Med Phys. 2012;39(2):1079-91.

[60] Nyeng TB, Hoffmann L, Khalil AA, Knap MM, Moeller DS. PO-0884: Implementation of soft tissue match using daily CBCTs for lung cancer patients results in reduced dose to lung. Radiotherapy and oncology. 2014;111:S97-S8.
[61] Andersen MH, Moeller DS, Knap MM, Rasmussen AB, Joergensen MK, Khalil AA, et al. SP-0032: RTT implementation of daily online soft tissue match for lung tumours. Radiotherapy and oncology. 2014;111:S9-S10.
[62] Mao W, Riess J, Kim J, Vance S, Chetty IJ, Movsas B, et al. Evaluation of Auto-Contouring and Dose Distributions for Online Adaptive Radiation Therapy of Patients With Locally Advanced Lung Cancers. Pract Radiat Oncol. 2022;12(4):e329-e38.
[63] Zhang Y, Yue N, Su MY, Liu B, Ding Y, Zhou Y, et al. Improving CBCT quality to CT level using deep learning with generative adversarial network. Med Phys. 2021;48(6):2816-26.
[64] Boer CG, Fjellanger K, Sandvik IM, Ugland M, Engeseth GM, Hysing LB. Substantial Sparing of Organs at Risk with Modern Proton Therapy in Lung Cancer, but Altered Breathing Patterns Can Jeopardize Target Coverage. Cancers (Basel). 2022;14(6):1365.

Appendix A

TNM classification of stage III lung cancer

Classification by the TNM staging system relevant to stage III lung cancer, both SCLC and NSCLC.

Table A.1: Explanation of the classification of stage III NSCLC

T – Primary Tumor

T1 Tumor 3 cm or less in the greatest dimension. Surrounded by lung or visceral pleura, and has not invaded the main bronchus.

- T1a Tumor 1 cm or less in greatest dimension
- T1b Tumor between 1 cm and 2 cm in greatest dimension
- T1c Tumor between 2 cm and 3 cm in greatest dimension

T2 Tumor between 3 cm and 5 cm in greatest dimension, or with any of the following features: involves main bronchus but without involvement of the carina, invades visceral pleura, associated with atelectasis or obstructive pneumonitis that extends to the hilar region either involving the whole lung or just parts of it.

- T2a Tumor between 3 cm and 4 cm in greatest dimension
- T2b Tumor between 4 cm and 5 cm in greatest dimension

T3 Tumor between 5 cm and 7 cm in greatest dimension, or the tumor directly invades any of the following: chest wall, phrenic nerve, parietal pericardium, parietal pleura; or separate tumor nodule(s) in the same lobe as the primary.

T4 Tumor larger than 7 cm or of any size that invades any of the following: mediastinum, diaphragm, heart, trachea, great vessels, recurrent laryngeal nerve, vertebral body, esophagus, carina; or separate tumor nodule(s) in a different ipsilateral lobe to that of the primary.

N – Regional Lymph Nodes

N0 No regional lymph node metastasis

N1 Metastasis in ipsilateral peribronchial and/or ipsilateral hilar lymph nodes and intrapulmonary nodes, including involvement by direct extension.

N2 Metastasis in ipsilateral mediastinal and/or subcarinal lymph node(s)

M – Distant Metastasis

M0 No distant metastasis

Appendix B

HELSE BERGEN Haukeland universitetssjukehus	Trafikklysprotokoll for lungepasienter (C34)
Kategori: Kjerneaktiviteter - Pasientbehandling somatikk	Gyldig fra/til:29.03.2020/29.03.2021
Organisatorisk plassering: HVRHF - Helse Bergen HF - Avdeling for kreftbehandling og medisinsk fysikk - Medisinsk fysikk	Versjon: 1.00
Godkjenner: Britt Nygaard	Retningslinje
Dok. ansvarlig: Monica Straume, John-Vidar Hjørnevik, Tone Nybø	Dok.id: D59802

Denne prosedyren gjelder stadie 3 lungepasienter som er med i pulmDIBH-studien.

Ved behandling stilles det inn etter daglig CBCT som beskrevet i Bildeprotokoll Lunge.
OBS: Det skal i utgangspunktet behandles etter skjelettmatch av hensyn til normalvevsdoser.
OBS OBS: Når det er endringer ved første fraksjon: Vurdèr å utsette behandlingsstart fremfor å starte behandling på en suboptimal plan

Vurdering av dagens CBCT ender i ett av fire aksjonsnivå:

Aksjons-nivå	Farge-kode	Beskrivelse	Aksjon
1		Store endringer, behandling gis ikke på nåværende plan	Ring 974057 (apparatfysiker)
2		Anatomiske endringer, dosedekke må vurderes	Task: Ktr.CBCT eller ktr.CT (behandling gis denne dag)
3		Noe endringer, antar dosedekke er greit	Noter hvilken type endring du ser
4		Små eller ingen endringer	Markèr med grønt

Tabell 1: Aksjonsnivå

Det noteres hvilken type endring man observerer etter tabell 2 (under).

Type endring	Kode	Kommentar
Atelaktase	A	*Sammenfalt lungevev*
Pleuravæske	P	
Infiltrative changes	I	*Interstitielle forandringer, fortetninger, fibrose*
Base line shift	B	*Tumorskift relativt til bein*
Tumorvekst	TV	
Tumor minket	TM	

Tabell 2: Koder for de aktuelle typer endringer

Farge- og type endring markeres i behandlingskort ved signatur for dagens behandling (se figur 1).

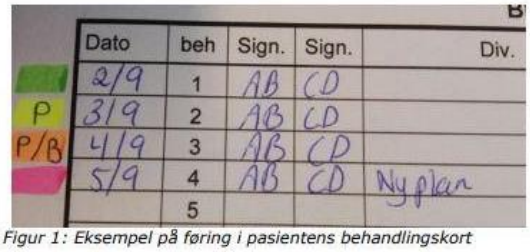

	Dato	beh	Sign.	Sign.	Div.
	2/9	1	AB	CD	
P	3/9	2	AB	CD	
P/B	4/9	3	AB	CD	
	5/9	4	AB	CD	Ny plan
		5			

Figur 1: Eksempel på føring i pasientens behandlingskort

Veiledning til vurdering

■ er når endringer gjør at man ikke kan treffe både tumor og lymfeknuteområde. Setupmargin fra ITV til PTV er 5 mm, både for tumor og lymfeknuter.

ATELAKTASE
Atelaktase kan være i endring under strålebehandling, og oppstår ofte i relasjon til tumor [1]. «Størrelse» på atelaktase kan ikke forutsi om replanlegging er nødvendig, men iflg. [1] vil 70% av alle atelaktaser kreve replanlegging, både på grunn av tumorskift og dosimetriske endringer. I utgangspunktet vil atelaktaser i tumorområdet alltid være ■.

PLEURAVÆSKE
Endring i pleuravæske alene førte ikke til skift i tumorposisjon [1].
Endring i pleuravæske kan påvirke dosen dersom feltinngang går gjennom pleuravæsken, men endring < 2 cm har lite å si for dosefordelingen[1].

- < 0.5 cm = □
- 0.5-2 cm = □
- > 2 cm = ■

INFILTRATIVE CHANGES - DIFFUSE TETTHETSENDRINGER
Oppstår ikke nødvendigvis i relasjon til tumor [1]. Diffuse tetthetsendringer i seg selv gir ikke grunnlag for replanlegging.

Diffuse tetthetsendringer i CBCT
- Hvis du ser tetthetsendringer som ikke påvirker tumorposisjon er dette □
- Hvis du lurer på om det kan være endring i tumormasse og det er innenfor PTV er det ■
- Hvis du lurer på om det er tilkommet tumormasse som er utenfor PTV er det □

BASE LINE SHIFTS
(= skift av tumorposisjon i forhold til beinmatch). I følge [1] krever systematiske base line shifts replanlegging. Om man matcher på tumor for å

treffe bedre mister man kontroll over dose til risikoorganer og må være særlig OBS på dose til medulla.
Base line shift

- < 2 mm = ☐ (diskuteres! Vi bruker gult for å fange opp endringer som kan bety noe for proton)
- 2-5 mm = ☐ (hold beinmatch!)
- > 5 mm = ☐ (*kan* etterjustere for tumorposisjon så tumor kommer innenfor PTV, men vær OBS på CTV lymfeknuter og dose til medulla)
- Base line skift som gjør det umulig å treffe både tumor og lymfeknuter = ☐

TUMORVEKST

- Tumor innenfor PTV samtidig som man treffer lymfeknuter = ☐
- Tumor kant-i-kant med PTV = ☐
- Tumor utenfor PTV = ☐

TUMOR MINKET

I utgangspunktet vil tumor fremdeles være godt dekket, og med tanke på eventuell subklinisk sykdom er det ikke gitt at CTV skal innskrenkes. MEN: Bortfall av fast tumormasse i lunge kan gi potensielle hotspots i normalvev.
Tumor krympet med:

- 1-3 cm = ☐
- > 3 cm = ☐
- Grenser diskuteres

Referanseliste

[1] Møller *et al,* Adaptive radiotherapy of lung cancer patients with pleural effusion or atelactasis, Radiotherapy and Oncology 110 (2014) 517-522